CD36-specific antibodies block release of HIV-1 from infected primary macrophages and its transmission to T cells

Stefano Berre,[1,2] Raphaël Gaudin,[1,2] Bruna Cunha de Alencar,[1,2] Marion Desdouits,[1,2] Mélanie Chabaud,[1,2] Nadia Naffakh,[3] Marc Rabaza-Gairi,[1,2] François-Xavier Gobert,[1,2] Mabel Jouve,[1,2] and Philippe Benaroch[1,2]

[1]Institut Curie, Centre de Recherche, F-75248 Paris, France
[2]INSERM U932, F-75248 Paris, France
[3]CNRS URA 3015, Institut Pasteur, 75724 Paris Cedex 15, France

HIV-1–infected macrophages likely represent viral reservoirs, as they accumulate newly formed virions in internal virus-containing compartments (VCCs). However, the nature and biogenesis of VCCs remain poorly defined. We show that upon HIV-1 infection of primary human macrophages, Gag is recruited to preexisting compartments containing the scavenger receptor CD36, which then become VCCs. Silencing of CD36 in HIV-1–infected macrophages decreases the amount of virions released. Strikingly, soluble anti-CD36 antibodies, but not the natural ligands of CD36, inhibit release of virions from HIV-1–infected macrophages and the transmission of virus to CD4$^+$ T cells. The effect of the antibodies is potent, rapid, and induces the retention of virions within VCCs. Ectopic expression of CD36 in HeLa cells renders them susceptible to the inhibitory effect of the anti-CD36 mAb upon HIV-1 infection. We show that the anti-CD36 mAb inhibits HIV-1 release by clustering newly formed virions at their site of budding, and that signaling via CD36 is not required. Thus, HIV-1 reservoirs in macrophages may be tackled therapeutically using anti-CD36 antibodies to prevent viral dissemination.

CORRESPONDENCE
P. Benaroch:
benaroch@curie.fr

Abbreviations used: EM, electron microscopy; LDL, low density lipoprotein; LDLR, LDL receptor; MOxLDL, mildly oxidized LDL; p.i., post infection; SIV-VLP, simian immunodeficiency virus–like particle; VCC, virus-containing compartment.

Early after its discovery, it has been established that HIV-1 infects not only CD4$^+$ T lymphocytes but also macrophages, like other lentiviruses. The presence of HIV-1–infected macrophages in vivo has been documented in various tissues (Gyorkey et al., 1985; Koenig et al., 1986; Pomerantz et al., 1988; Jarry et al., 1990). The precise contribution of macrophages to the infection and pathogenesis of HIV-1 still remains to be established. Nevertheless, macrophages are considered as viral reservoirs because they are long-lived cells resistant to the cytopathic effects of HIV-1. Indeed, HIV-1–infected macrophages can survive for months (Salahuddin et al., 1986; Orenstein et al., 1988) and store infectious virions for extended periods of time (Sharova et al., 2005). Supporting the idea of a viral reservoir in macrophages, newly formed virions are assembled and stored in unusual intracellular compartments, often referred to as virus-containing compartments (VCCs; Tan and Sattentau, 2013), which may protect virions from the immune response and antiviral drug treatments.

The VCC appears to be a macrophage-specific compartment, clearly distinct from the endocytic pathway as it possesses a neutral pH (Jouve et al., 2007) and expresses a subset of endocytic markers such as CD81 and CD9 but not Lamp1 nor Lamp2 (Pelchen-Matthews et al., 2003; Marsh et al., 2009). Moreover, its limiting membrane is often decorated by a thick molecular coat, which contains β2 integrins (Pelchen-Matthews et al., 2012) and members of the

R. Gaudin and B.C. de Alencar contributed equally to this paper.
S. Berre's present address is Institut Pasteur, INSERM U1117, 75724 Paris Cedex 15, France.
R. Gaudin's present address is Program in Cellular and Molecular Medicine at Children's Hospital, Boston, MA 02115.

The Rockefeller University Press $30.00
J. Exp. Med. 2013 Vol. 210 No. 12 2523-2538
www.jem.org/cgi/doi/10.1084/jem.20130566

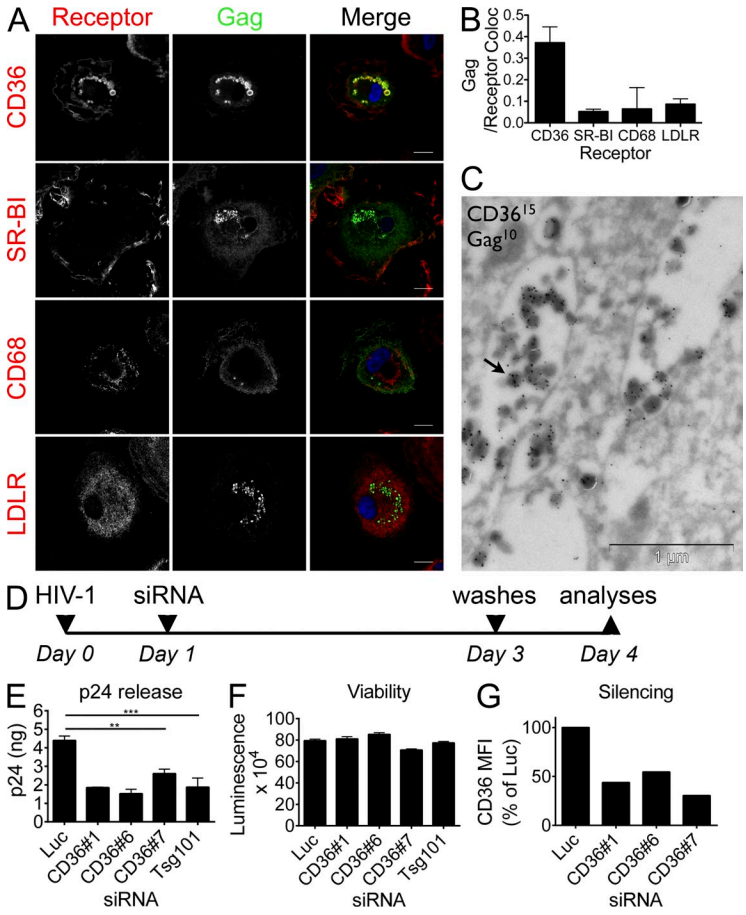

Figure 1. CD36 is present in the VCC and is required for efficient HIV-1 release by primary macrophages. (A) Confocal sections of macrophages infected with HIV-1 NLAD8 for 7 d and stained for the indicated markers. Merge images include DAPI staining in blue. Bars, 10 µm. (B) Quantification of the codistribution of Gag with the receptors imaged in A. For each cell, mean Pearson's coefficient was calculated and for each group ($n > 15$), data are presented as geometric mean with 95% C.I. (C) Immuno-EM of HIV-1–infected macrophages. Ultrathin cryosections were double labeled for p17 Gag with PAG 10 (Protein A coupled to gold particles of 10 nm diameter) and for CD36 with PAG15. The arrow indicates a viral particle stained with both anti-CD36 and anti-p17 Gag antibodies. (D) Schematic representation of the experimental design. (E) Measurement of p24 Gag released in the supernatant of macrophages that had been infected with HIV-1 and transfected with the indicated siRNA. Washes were performed at day 3. Supernatants were collected 24 h after and analyzed by ELISA for their p24 Gag content. Data are presented as mean ± SEM of four replicates. One-way ANOVA with Tukey's Multiple Comparison Test was used as statistic test (**, $P \leq 0.01$; ***, $P \leq 0.001$). (F) Cell viability determined at the end of the experiments using CellTiter-Glo is expressed in arbitrary units of luminescence and presented as mean ± SEM of four replicates. (G) Silencing efficiency was estimated by flow cytometry analysis of the various cell populations that were fixed and stained for CD36. MFI is expressed as percentage of the control (cells transfected with siRNA specific for luciferase). Images are representative of at least two independent experiments. Experiments depicted in E and F have been repeated at least three times with different donors, and twice for the one in G.

ESCRT (endosomal sorting complexes required for transport) machinery (Benaroch et al., 2010). Although the exact origin and nature of the VCC remains obscure so far, indirect evidence suggests that VCCs represent specialized domains of the plasma membrane that have been sequestered intracellularly (Deneka et al., 2007; Welsch et al., 2007). Supporting this plasma membrane origin, VCCs can remain accessible to the external medium through conduits or narrow microchannels (Deneka et al., 2007; Welsch et al., 2007; Bennett et al., 2009). One third of the VCCs are accessible to the external medium overtime, but this access can be transient and therefore suggests that such connections are dynamic (Gaudin et al., 2013). VCCs evolve with time post infection (p.i.) as the density of viral particles present in their lumen increases (Gaudin et al., 2013). Such compartments are absent from T lymphocytes where viral assembly takes place at the plasma membrane. In macrophages, HIV-1 assembly occurs at the limiting membrane of the VCCs through mechanisms that remain to be deciphered (Tan and Sattentau, 2013).

To approach these mechanisms, we examined the role of proteins specific for macrophages as compared with T lymphocytes. More precisely, we looked for macrophage proteins that could potentially be involved in the functioning of the VCC and may represent targets to treat the intracellular stocks of virus present in the infected macrophages. Macrophages are equipped with a collection of phagocytic receptors (including lectins, integrins, GPI-anchored proteins, and scavenger receptors) that allow the internalization of many self-, nonself-, or modified self-components such as modified low density lipoproteins (LDLs; Taylor et al., 2005). We focused on the scavenger receptor family, which is highly expressed in monocytes/macrophages as compared with T lymphocytes (Areschoug and Gordon, 2009). CD36 belongs to the class B scavenger receptor family and is expressed by endothelial cells, smooth muscle cells, adipocytes, platelets, and macrophages but not by T lymphocytes (Talle et al., 1983; Swerlick et al., 1992; Matsumoto et al., 2000; Kuniyasu et al., 2003). In macrophages, it binds to multivalent ligands such as oxidized LDL, components of the bacterial surface, and apoptotic cells (Savill et al., 1992; Endemann et al., 1993; Hoebe et al., 2005; Stuart et al., 2005).

Here, we show that HIV-1 hijacks preexisting $CD36^+$ compartments for its own assembly in macrophages. Exposure to CD36-specific antibodies inhibits virus release due to retention into VCCs. This effect is rapid, potent, long lasting, and does not require signaling through the known pathway of CD36 signal transduction. Our results further suggest that exposure to CD36 antibodies induces a tethering of virions within VCCs thereby inhibiting their release and transmission to $CD4^+$ T lymphocytes.

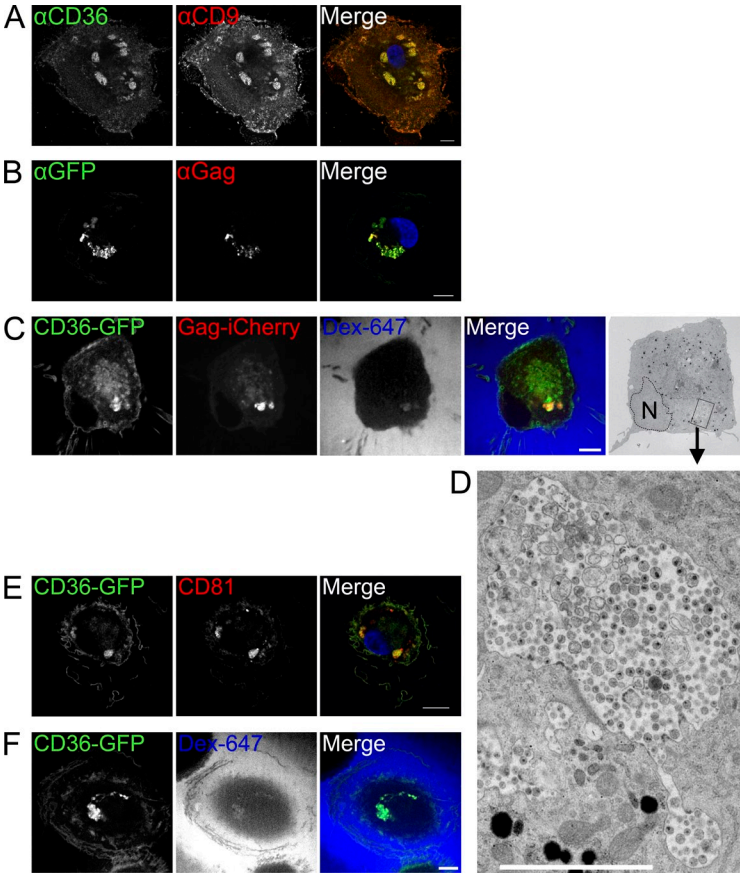

Figure 2. Plasma membrane–connected CD36⁺ compartments are present in infected and uninfected macrophages. (A) Confocal micrographs of uninfected macrophages stained for the indicated antibodies. (B) Confocal sections of primary macrophages co-infected with HIV-1 Gag-iCherry ΔEnv and CD36-GFP lentiviral vector for 7 d, fixed, and stained for the indicated markers. In B and E anti-GFP antibodies were used to enhance the GFP signal. (C) Macrophages grown on fluorodishes with coordinates were infected with a lentiviral vector encoding CD36-GFP, together with SIV-VLP and, 5 d later, with HIV-1 Gag-iCherry ΔEnv. On day 7 p.i., cells were exposed to a 10 kD dextran–Alexa Fluor 647 and then immediately imaged by spinning disk microscopy to follow the indicated markers. The same fluorodishes were then embedded in epon resin and processed for EM. An overview of the macrophage imaged by EM is presented on the right. N = nucleus. (D) Magnification of the region boxed on the right, with viral budding profiles visible at the limiting membrane and both mature and immature viral particles. (E) Macrophages infected with the lentiviral vector encoding CD36-GFP for 7 d were fixed and stained for the VCC marker CD81. (F) Macrophages infected with the lentiviral vector encoding CD36-GFP for 12 d were exposed as in C to dextran–Alexa Fluor 647 and then immediately imaged by spinning disk microscopy. In A, B, and E merge images include DAPI staining in blue. Data shown are representative of at least two independent experiments. Bars: (A–C, E, and F) 10 µM; (D) 2 µM.

RESULTS

The VCC in HIV-1–infected macrophages contains CD36 but no other LDL receptors (LDLRs)

To approach the potential involvement of host factors in the macrophage-specific location of HIV-1 assembly, we first analyzed, in HIV-1–infected macrophages at 7 d p.i., the intracellular distribution of three scavenger receptors and of the classical LDLR with respect to Gag localization by immunofluorescence (Fig. 1 A). We observed that staining specific for SR-BI, CD68, and LDLR was distinct from the one of Gag. In contrast, CD36 staining was not only present in membrane ruffles of the plasma membrane but also in internal compartments that stained positive for Gag (Fig. 1, A and B for quantifications) and for Env (not depicted), indicating that CD36 is associated with VCCs. Furthermore, analysis of infected macrophages at the ultrastructural level by immuno–electron microscopy (EM) revealed the presence of CD36 on Gag⁺ virions present in the lumen of VCCs (Fig. 1 C). We conclude that CD36 is associated with the VCCs and virions in HIV-1–infected macrophages.

CD36 expression is required for HIV-1 release by macrophages

The potential involvement of CD36 during the HIV-1 cycle in macrophages was evaluated by CD36 silencing. HIV-1–infected macrophages were transfected with siRNAs specific for CD36, luciferase as a negative control, and Tsg101 as a positive control (Fig. 1 D, scheme). CD36 silencing using three different siRNAs specific for CD36 led to a strong reduction (up to 65%, $P \leq 0.001$ for the three siRNA on three independent experiments) of the amount of p24 Gag secreted in the supernatant (Fig. 1 E). The extent of the inhibition was similar to the one obtained upon silencing of Tsg101, an ESCRT protein crucial for viral budding (Garrus et al., 2001). Cell viability was similar in the different cell populations (Fig. 1 F). Efficiency of CD36 silencing ranged from 50 to 70% as determined by intracellular FACS staining (Fig. 1 G). Analysis of the kinetics of the inhibitory effect of CD36 silencing on p24 Gag release revealed that it was clearly visible at days 2–3 and 3–4 (65 and 48% reduction, respectively, for siRNA CD36#6; not depicted). In contrast, intracellular Gag levels measured at day 4 were not altered in any condition (not depicted). We conclude that CD36 expression is required for efficient release of HIV-1 particles by infected macrophages.

CD36⁺ compartments remain accessible to the external medium in uninfected and infected macrophages

The presence of CD36 in the VCCs raised the question of the existence of similar compartments before HIV-1 infection. In uninfected macrophages, we observed that CD36⁺ compartments were CD9⁺ (Fig. 2 A) and Lamp1⁻ (not depicted), similar to VCCs in infected macrophages (Raposo et al., 2002;

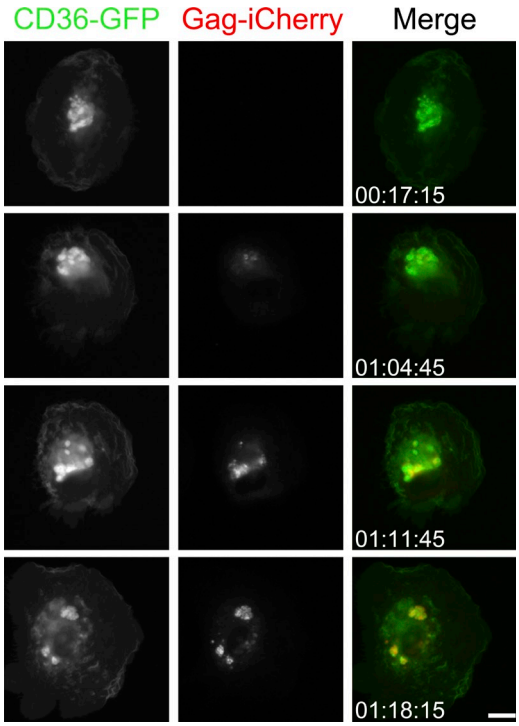

Figure 3. Upon HIV-1 infection, Gag is recruited to preexisting CD36⁺ compartments in macrophages. Macrophages were first transduced with a lentivector encoding CD36-GFP and, 4 d later, infected with HIV-1 Gag-iCherry ΔEnv. After another 8 h, cells were washed and then live imaged during 2 d (see Video S1). The presented images were acquired at the indicated time (days:hours:minutes). Bar, 10 µM.

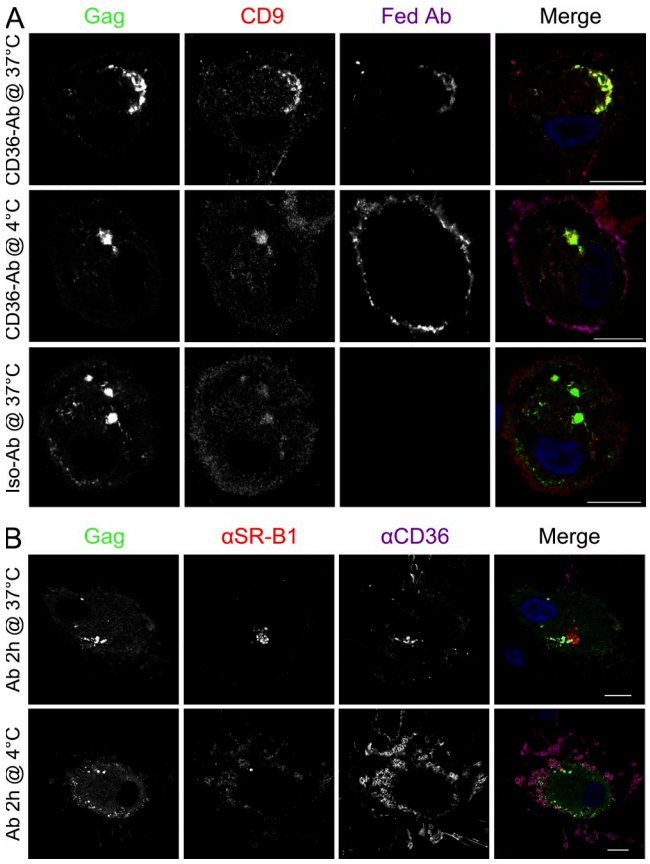

Figure 4. Exogenously added antibodies specific for CD36 are transported into the VCC. (A) Confocal micrographs of HIV-1 Gag-iGFP–infected primary macrophages are presented. Cells were exposed for 2 h at 37 or 4°C with the indicated mAb, then fixed and stained for CD9, whereas isotype control mAbs as well as CD36-specific mAbs were revealed with appropriate secondary antibodies (Bars, 10 µM). (B) Confocal micrographs of HIV-1 Gag-iGFP–infected macrophages simultaneously exposed to antibodies specific for SR-BI (rabbit antibodies) and CD36 (mouse mAb) for 2 h. Both types of antibodies are internalized at 37°C (not at 4°C), but only the CD36-specific mAb colocalizes with Gag⁺ compartments. Merge images include DAPI staining in blue. Data shown are representative of two independent experiments. Bars, 10 µM.

Pelchen-Matthews et al., 2003; Deneka et al., 2007; Jouve et al., 2007). To perform additional characterization of the CD36 compartments, we built a lentivector encoding CD36-GFP, a fusion protein known to be functional (Zhang and Crandall, 2007). CD36-GFP co-distributed with endogenous CD36 (not depicted) and in HIV-1–infected macrophages, with Gag (Fig. 2 B).

These results further suggested that CD36⁺ compartments in uninfected and infected macrophages were related. One of the major specific features of the VCC being its accessibility to external medium, we tested whether CD36⁺ VCC shared this property. Live macrophages co-infected with the lentivector CD36-GFP and HIV-1 Gag-iCherry ΔEnv were imaged before and immediately (in less than 10 s) after exposure to a fluorescent fluid phase marker, a 10-kD Dextran–Alexa Fluor 647 (Dex-647), as recently described (Gaudin et al., 2013). We observed that Dex-647 was able to access CD36⁺ VCCs (see the large Gag⁺CD36⁺Dex-647⁺ compartment at the bottom of the cell in Fig. 2 C). Moreover, correlative EM performed on the very same cell established that this compartment contained both mature and immature viral particles (Fig. 2 D) and was therefore a bona fide VCC. Similar experiments performed on uninfected macrophages expressing CD36-GFP revealed that internal CD36⁺ compartments were also CD81⁺ (Fig. 2 E) and accessible to Dex-647 (Fig. 2 F).

We conclude that CD36⁺ internal compartments in uninfected and infected macrophages share markers and possess plasma membrane connections allowing passive diffusion of small compounds.

Gag accumulates in preexisting CD36⁺ compartments

These results prompted us to investigate whether HIV-1 could subvert preexisting CD36⁺ compartments and convert them into VCCs. Primary macrophages were infected first with the CD36-GFP lentivector together with simian immunodeficiency virus–like particles (SIV-VLPs) containing Vpx to increase the rate of infection (Goujon et al., 2008) and 4 d later with HIV-1 Gag-iCherry ΔEnv. Cells were imaged at day 0.5 after HIV addition by time-lapse epifluorescent microscopy at a rate of one image every 15 min for 2 d. At early

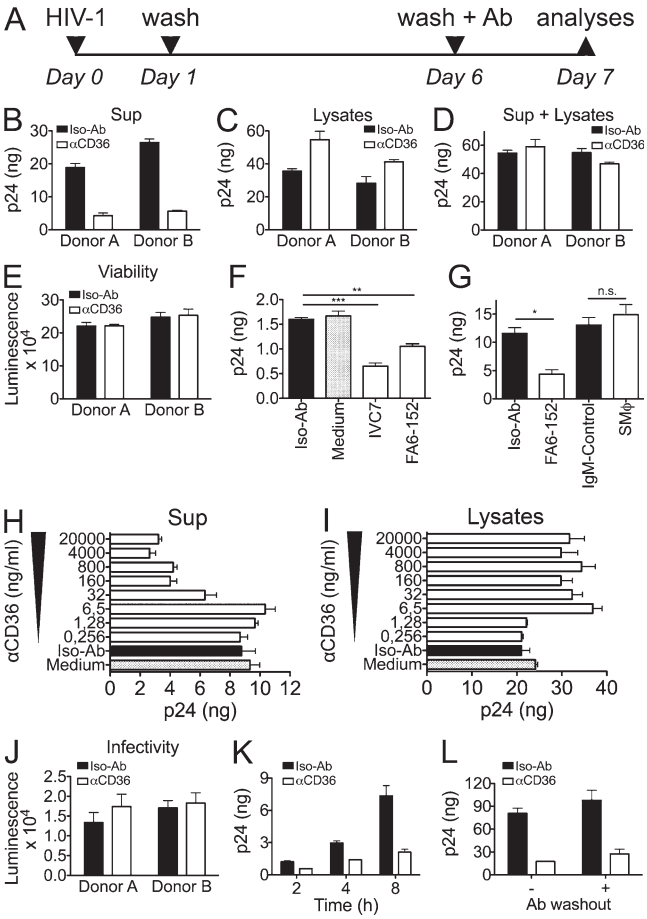

Figure 5. CD36-specific antibodies induce a potent, rapid, and long-lasting inhibition of HIV-1 release from macrophages. (A) Schematic representation of the experimental design. (B and C) Quantification of p24 Gag present in the overnight culture supernatant harvested as indicated in A (B), and in the corresponding cell lysates (C). (D) Total p24 Gag found in the supernatant + the cell lysates. (E) Cell viability was measured at the end of the experiment with the CellTiter-Glo kit. (F and G) Quantification of p24 Gag released from primary macrophages treated overnight with the indicated Abs. In F, all antibodies were used at 1 µg/ml. In G, the IgM specific for CD36 (SMΦ) was used, like its isotype control, at 20 µg/ml, while the FA6-156 and its isotype control were used at 10 µg/ml. (H and I) Titration of the effect of CD36-specific mAb (clone IVC7) on HIV-1–infected macrophages on the amounts of secreted (H) and cell-associated (I) p24 Gag. (J) Infectivity of the virions on the reporter cell line TZM-bl produced by the macrophages subjected to the anti-CD36 mAb treatment was evaluated using the same amount of p24 Gag (10 ng/ml; see Materials and methods). (K) Quantification of p24 Gag in the supernatant of HIV-1 NLAD8-infected macrophages treated at 7 d p.i. with an anti-CD36 mAb (FA6-152) or its isotype control for the indicated time. (L) Quantification of the p24 Gag produced by HIV-1 NLAD8–infected macrophages in a 24-h time window before (−) or after (+) antibody washout. 6-d-infected macrophages were washed and exposed to the indicated antibodies for 24 h. Then cells were washed out and incubated in compete medium for another 24 h. Supernatant collected before and after antibody washout were stored at −20°C for at least 1 d before p24 Gag quantification. Representative experiments are presented in B–L. All the experiment have been reproduced at least three times with three different donors, except for H and I, which have been performed once (similar results are shown in Fig. 6 I).

time points, CD36-GFP was observed in cells that were devoid of Gag, and was present at the plasma membrane and in intracellular compartments (Fig. 3). With time, some macrophages exhibited a diffuse Gag-iCherry signal in the cytosol which then became concentrated in internal compartments, most of them being CD36-GFP$^+$ (Fig. 3). We also unambiguously witnessed Gag recruitment and accumulation in preexisting CD36-GFP$^+$ structures (Fig. 3 and Video 1). We conclude that Gag accumulates in preexisting CD36$^+$ compartments in infected macrophages.

Targeting VCCs in macrophages with a CD36-specific mAb

CD36 is a receptor located at the plasma membrane that is internalized in macrophages after ligand recognition (Zeng et al., 2003; Collins et al., 2009). We first established that CD36-specific antibodies when incubated for 2 h at 37°C with uninfected macrophages are able to reach internal CD81$^+$ compartments (unpublished data). We therefore asked whether CD36 antibody is also internalized in infected macrophages and if it can reach VCCs. To address these questions, HIV-1–infected macrophages were exposed to a mAb specific for CD36 at 37°C for 2 h. After fixation and appropriate staining, cells were analyzed by confocal microscopy. The CD36-specific mAb was able to access Gag$^+$CD9$^+$ compartments, whereas an isotype control used in the same conditions could not (Fig. 4 A). Incubation at 4 instead of 37°C prevented the CD36 mAb to access VCCs (Fig. 4 A), and stained regions of the plasma membrane. Moreover, simultaneous exposure of HIV-1–infected macrophages to antibodies specific for SR-B1 and CD36 at 37°C for 2 h led to the specific accumulation of the CD36 mAb into Gag$^+$ compartments (Fig. 4 B). SR-B1 antibodies were also internalized but in intracellular compartments clearly distinct from the Gag$^+$ ones. Such transport did not occur at 4°C for both types of antibodies. These data show that anti-CD36 mAb can be actively and specifically transported into VCCs in HIV-1–infected macrophages.

CD36-specific mAb inhibits HIV-1 release by infected macrophages

The accessibility of the VCCs to exogenously added CD36-specific mAb prompted us to investigate the effect of such antibodies on HIV-1 release by infected macrophages (Fig. 5 A, experimental design). Exposure of HIV-1–infected macrophages to CD36-specific mAb for 24 h led to a strong reduction (80% mean, $P \leq 0.001$ in three independent experiments) of the amounts of p24 Gag released in the supernatant as compared with macrophages exposed to an isotype control antibody (Fig. 5 B). Conversely, the amounts of p24 Gag detected in the corresponding cell lysates increased (40% mean, $P \leq 0.001$ in three independent experiments) in anti-CD36–treated cells as compared with isotype-treated cells (Fig. 5 C).

Data are shown as mean ± SEM of triplicates. One-way ANOVA with Tukey's multiple comparison test was used as a statistical test (*, $P \leq 0.05$; **, $P \leq 0.01$; ***, $P \leq 0.001$).

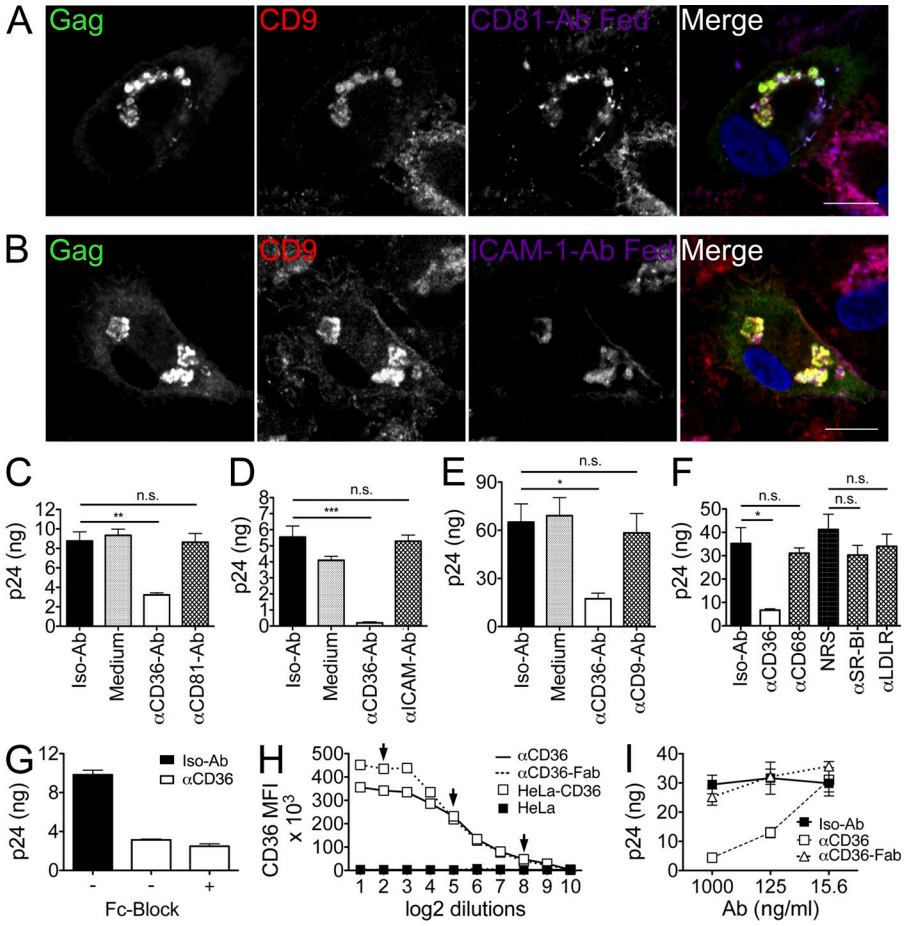

Figure 6. The anti-CD36–mediated inhibition of HIV-1 release is specific and requires bivalent binding. (A and B) Exogenous CD81 and ICAM-1–specific antibodies are transported to the VCC. Macrophages were infected with HIV NLAD8 for 3 d, washed, and incubated for 2 h with a CD81-specific mAb (A) or an ICAM-1–specific mAb (B). mAbs were used at a final concentration of 5 µg/ml. Cells were then washed, fixed, permeabilized, and stained for Gag and CD9 to identify VCCs. Bars, 10 µm. Merge images include DAPI staining in blue. (C–F) Quantification of p24 Gag released from macrophages treated overnight with the indicated antibodies. Of note, other antibodies transported to the VCC (C and D), antibodies specific for markers of the VCC (C, D and E), and antibodies specific for other LDLRs (F) did not modulate HIV-1 release from macrophages. (G) Quantification of the p24 Gag produced by HIV-1–infected primary macrophages treated (as indicated in Fig. 5 A) with the FA6-152 antibody in the presence or not of Fc-blocking antibodies. (H) Flow cytometry titration of the anti-CD36 mAb CLB-IVC7 and its Fab fragment. HeLa-CD36 (open symbols) and HeLa cells (black symbols) were stained with serial dilutions of the anti-CD36 mAb and its Fab revealed by appropriate secondary antibodies. MFIs are plotted as a function of the Ab dilutions. (I) Quantification of p24 Gag released from macrophages treated overnight with the anti-CD36 mAb, its Fab fragment, or the isotype control. Cells were exposed to the three dilutions indicated by arrows in H. Data are shown as mean ± SEM of triplicates. In C–I, representative experiments are shown. All the experiments have been reproduced at least two times with different donors. One-way ANOVA with Tukey's multiple comparison test was used as a statistical test (*, $P \leq 0.05$; **, $P \leq 0.01$; ***, $P \leq 0.001$).

As a result, the sum of the amount of p24 Gag found in the supernatant and corresponding cell lysates in each of the conditions remained roughly constant (Fig. 5 D). These antibody exposures did not have any effect on the cell viability (Fig. 5 E). Two CD36-specific mAbs, FA6-152 and CLB-IVC7, induced a potent inhibition of p24 Gag release (Fig. 5 F), indicating that the effect observed was not a peculiarity of a single mAb. In contrast, SMΦ, an IgM mAb also specific for CD36, did not affect p24 Gag release from macrophages (Fig. 5 G). Of note, we verified that SMΦ antibody binds CD36 by flow cytometry (unpublished data).

Titration revealed that as little as 32 ng/ml CLB-IVC7 (a CD36-specific mAb) was sufficient to induce a 30% reduction of the p24 Gag released in the culture supernatant of infected macrophages (Fig. 5 H). This inhibition was accompanied by an increase in the amount of p24 Gag found in the corresponding cell lysates (Fig. 5 I). Despite the presence of CD36 on the virions (Chertova et al., 2006; Fig. 1 B), addition of the anti-CD36 mAbs at similar concentrations used in the assays above (2 µg/ml) did not affect the capacity of the virions to infect reporter TZM-bl cells (not depicted). The anti-CD36 treatment did not affect the infectivity of the few virions still released, as measured using normalized amounts of p24 Gag (Fig. 5 J). This indicates that the measurement of the p24 Gag level reflects the amount of infectious virions released.

The inhibitory effect of the anti-CD36 mAb on p24 Gag release was already detectable after 2 h of antibody exposure (Fig. 5 K), suggesting a rapid mechanism probably independent of protein synthesis. Furthermore, we observed that a 1-d anti-CD36 mAb exposure followed by a 1-d culture in mAb-free medium still strongly inhibited the p24 Gag release by macrophages during the subsequent 24 h (Fig. 5 L). This suggested that the effect induced was long lasting and confirmed that it did not result from the neutralization of the released virions but rather from an effect at the cellular level, possibly within the VCCs. We conclude that exposure of infected macrophages to soluble anti-CD36 antibodies are sufficient to strongly inhibit HIV-1 release.

Inhibition of HIV-1 release is specific to anti-CD36 mAbs and requires bivalent antibodies

VCCs as well as viral particles are enriched in many host proteins such as the CD81 tetraspanin and the ICAM-1 adhesion

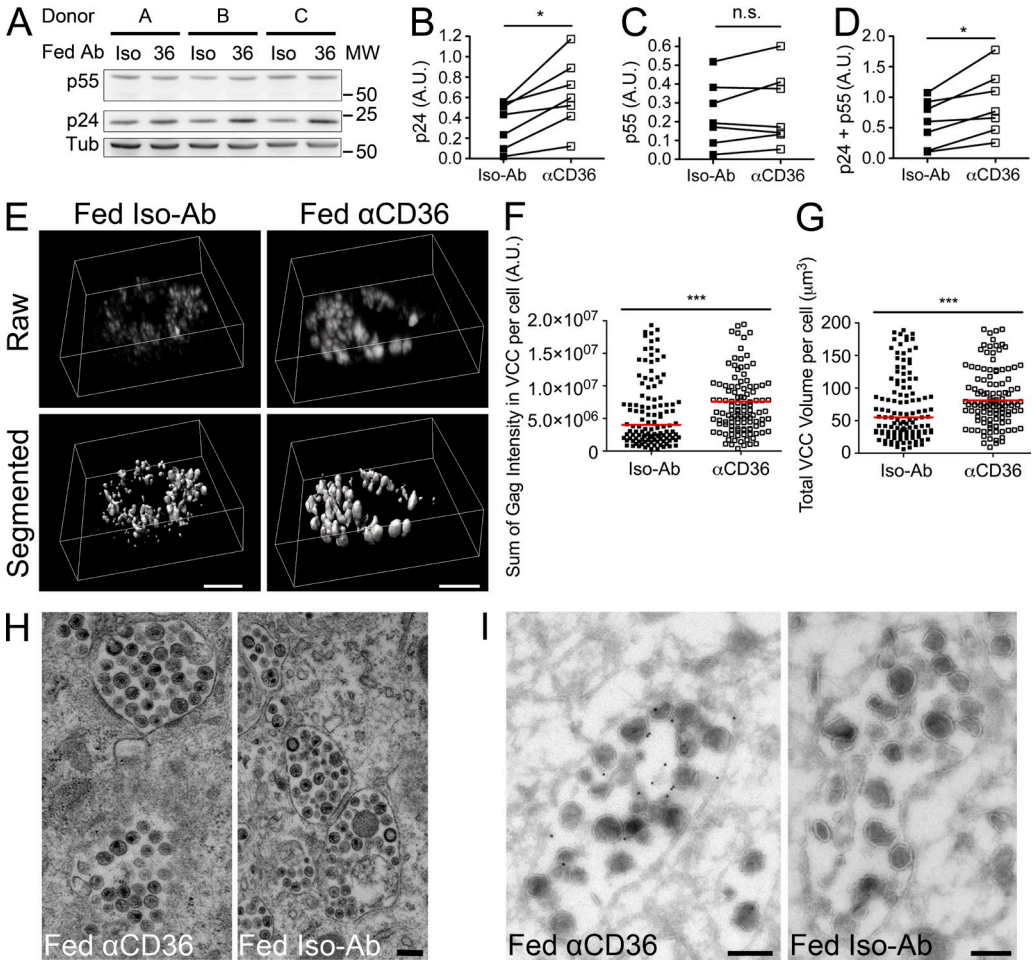

Figure 7. Exposure to CD36-specific antibodies induces intracellular accumulation of virions in VCCs. (A) Immunoblot analysis of Gag polypeptides present in lysates of infected macrophages exposed to the CD36 mAb (36) or its isotype control (Iso). Bands corresponding to p55 Gag (p55), p24 Gag (p24), and tubulin (Tub) are indicated. The molecular weight corresponding to the closest band of the ladder is indicated. (B–D) Quantifications of the intensity of the various Gag polypeptides present in cell lysates were performed by immunoblot analysis as in A. The experiments were repeated with cells from seven donors. p55 Gag and p24 Gag signals were normalized for α-tubulin. Statistical analyses were performed using the Wilcoxon matched pairs test (*, $P \leq 0.05$). (E) Examples of 3D reconstructions obtained before and after segmentation of image stacks acquired by confocal microscopy of macrophages infected with HIV-1 Gag-iGFP for 7 d, and exposed from days 5 to 7 to the anti-CD36 mAb or its isotype control. Bars, 7 µm. Segmented reconstructions, as seen in E, were quantified using Imaris software. Graphs illustrating the variation of the total Gag intensity per cell (F) and the total volume of VCC per cell (G) are presented. Effect of the anti-CD36 on p24 Gag release was estimated in parallel by Elisa in the three donors used for these experiments. The mean inhibition of p24 Gag release was 90%. Data are presented with the median in red. Each square corresponds to a cell. Statistical analyses were performed using the Mann-Whitney test (***, $P \leq 0.001$). (H) HIV-1 NLAD8–infected macrophages at 6 d p.i. were washed and treated with anti-CD36 mAbs or with its isotype control for 48 h. Cells were then fixed, embedded in epon, and processed for EM. Bar, 200 nm. (I) HIV-1–infected macrophages treated as in H were prepared for immuno-EM. mAbs present in internal compartments were detected with appropriate secondary antibodies revealed by PAG10. Bars, 200 nm. Representative images are shown in H and I. Data were reproduced with three different donors.

molecules, in addition to CD36 itself (Chertova et al., 2006). To evaluate whether the inhibition of virion release was restricted to CD36-specific antibodies, similar experiments were performed using other antibodies. Antibodies specific for CD81 and ICAM-1 accessed VCCs when added exogenously to infected macrophages at 37°C for 2 h (Fig. 6, A and B) but not at 4°C (not depicted). However, exposure to antibodies specific for CD81, ICAM-1, or CD9 did not modify the amounts of p24 Gag released by macrophages (Fig. 6, C–E), indicating that antibody access to the VCC was not sufficient to induce the retention of the virions. Similarly, exposure to antibodies specific for other lipid receptors, including scavenger receptors (CD68, SR-B1, or LDLR), did not modify the release of p24 Gag as compared with their respective isotype controls (Fig. 6 F).

Inhibition of HIV-1 release upon anti-CD36 mAb exposure remained unchanged in the presence of the FcR blocking reagent (Fig. 6 G), indicating that Fc receptors were not involved in the antibody-mediated effect. Exposure of HIV-1–infected macrophages to the Fab fragment prepared from the

CD36-specific CLB-ICV7 mAb (Fig. 6 H, comparative titration of the mAb and its Fab) at three concentrations (Fig. 6 H, arrows) did not affect p24 Gag release, in contrast to the inhibition observed with the bivalent mAb (Fig. 6 I). These results establish that the inhibitory effect of the anti-CD36 mAbs on p24 Gag release by infected macrophages is highly specific and requires bivalency.

Exposure to the anti-CD36 antibody leads to retention of virions into VCCs

To evaluate the impact of the anti-CD36 mAb exposure on the HIV-1 cycle, we first looked at the maturation of the Gag precursor. The precursor p55 Gag is synthesized as a cytosolic protein. Once within the newly formed virions, p55 Gag is cleaved into four main polypeptides, including the Capsid p24 Gag. Exposure to the anti-CD36 mAb induced an intracellular accumulation of p24 Gag in infected macrophages as measured by immunoblot (Fig. 7 A). Quantification of the amounts of p55 and p24 Gag in cells from seven donors was performed from immunoblot analyses. Results expressed as the amounts of p24, p55, or total Gag (Fig. 7, B–D, respectively) normalized for the tubulin levels confirmed that anti-CD36 mAb exposure led to the accumulation of cell-associated p24 Gag that represents, in all likelihood, virions.

These results were confirmed by quantification of 3D reconstruction images of antibody-treated infected macrophages (Fig. 7 E, examples). Different parameters were extracted, including the sum of the Gag fluorescence intensity present in VCCs per cell (Fig. 7 F) and the total volume of the VCCs per cell (Fig. 7 G), which were both increased upon antibody exposure (statistically significant $P \leq 0.001$).

EM analysis of anti-CD36– and isotype-treated infected macrophages revealed that both types of cells possessed VCCs containing mature and immature virions (Fig. 7 H). We also observed budding profiles at the limiting membrane of the VCCs under both conditions, suggesting that the antibody treatment did not affect the assembly process per se. Substantial amounts of anti-CD36 mAb were detected within VCCs of cells exposed to anti-CD36 mAb but not to the isotype control (Fig. 7 I). Interestingly, the staining appeared rather associated to the membranes of the virions, suggesting that the mAb may create a network through its binding to the CD36 present in the viral membranes. We conclude that the anti-CD36 mAb exposure induces the retention of virions within the VCCs of infected macrophages, increasing the volume of the VCCs and thus inhibiting the particle release to the extracellular medium.

The mildly oxidized LDL (MOxLDL)–CD36 pathway is not activated by the anti-CD36 mAb

Among the many ligands that CD36 can internalize in macrophages, MOxLDL has been widely studied (Endemann et al., 1993; Nozaki et al., 1995; Kunjathoor et al., 2002; Collins et al., 2009; Jaqaman et al., 2011). The effect of the anti-CD36 mAb could be related to the pathway induced by MOxLDL-CD36 interaction. To test this hypothesis, we first exposed HIV-1–infected macrophages to freshly thawed MOxLDL or to the anti-CD36 mAb or its isotype control for 10 or 30 min and measured the phosphorylation of JNK. As expected, MOxLDL induced via CD36 the expected JNK phosphorylation (Rahaman et al., 2006; Rios et al., 2012) after 10 min of exposure (Fig. 8 A), indicating that the MOxLDL used was biologically active. In contrast, anti-CD36 (or its isotype control) exposure had no effect on the levels of JNK phosphorylation, even after 30 min (Fig. 8 A), suggesting that conventional signaling through CD36 does not take place upon exposure to the CD36 mAb.

To evaluate the impact of MOxLDL exposure on the virus release, HIV-1–infected macrophages were exposed to biologically active MOxLDL together or not with the anti-CD36 mAb or its isotype control for 24 h. In all cases, the amount of p24 Gag measured in the supernatant was not modified by the presence of MOxLDL (Fig. 8 B) nor was the cell viability (Fig. 8 C).

We also tested whether the anti-CD36 mAb-mediated inhibition of virion release was dependent on the presence of LDLs in the culture medium. HIV-1–infected macrophages were starved for 4 h and then cultured for 24 h in medium complemented with lipoprotein-deficient serum, or without any fetal calf serum, and in the presence of the anti-CD36 mAb or its isotype control. In all cases the anti-CD36 mAb exposure led to a strong reduction in the amounts of p24 Gag secreted in the supernatant (Fig. 8 D). These data indicate that exposure to the anti-CD36 mAb does not induce a signaling pathway similar to the one induced by MOxLDL. Moreover, our data rule out the possibility that the anti-CD36 mAb effect on particle release is linked to MOxLDL interaction with CD36.

Besides MOxLDL, other endogenous ligands of CD36 include trombospondin 1 and type-I collagen (Asch et al., 1987; Tandon et al., 1989). We tested in a similar manner on infected macrophages whether overnight exposure to these two ligands exerts any effect on virion release. Although exposure to the anti-CD36 mAb induced a strong inhibition, none of the two ligands reduced the release of p24 Gag (Fig. 8 E). We checked that both ligands were biologically active on uninfected macrophages by analyzing the phosphorylation status of the JNK and Src kinases (Roberts et al., 2010; not depicted). Collectively, these data suggest that the anti-CD36 mAb effect on particle release is not related to the pathways induced upon CD36 binding to some of its endogenous multivalent ligands such as MOxLDL, trombospondin 1, or type-I collagen.

HeLa cells expressing CD36 are sensitive to the Ab effect

To get insight into the mechanism of action of the CD36 antibody, we needed to set up a more flexible cellular model than primary macrophages; thus, we derived HeLa cells expressing CD36. Stable expression of CD36 in HeLa cells did not modify the amounts of p24 Gag released upon HIV-1 infection (unpublished data). However, as observed with macrophages, exposure of HIV-1–infected HeLa-CD36 to CD36-specific mAb for 24 h led to a strong reduction (73% mean, $P \leq 0.001$ on three independent experiments) of the amounts

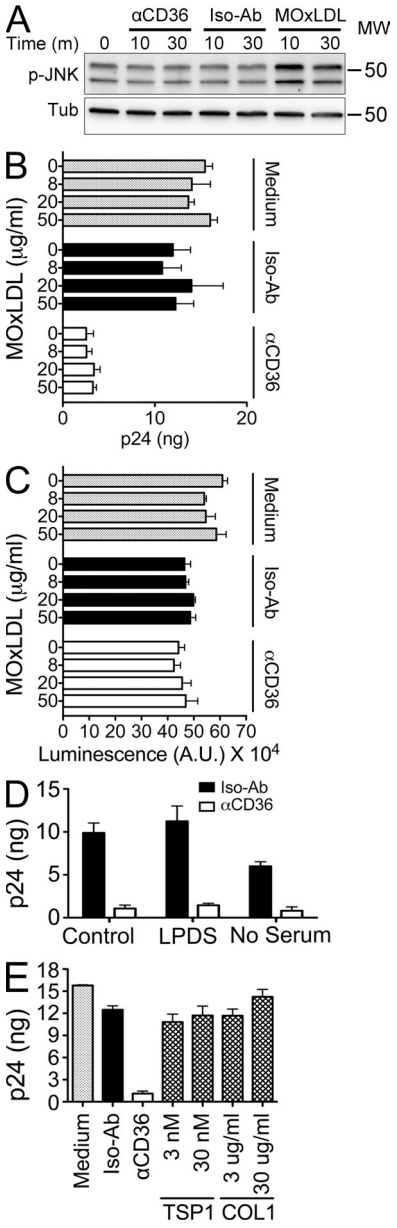

Figure 8. Modulation of HIV-1 release by anti-CD36 antibody exposure is not related to CD36 interaction with MOxLDL, TSP-1, or type-I collagen. (A) Immunoblot analysis of the phosphorylation of JNK after different stimuli. HIV-1 NLAD8-infected macrophages starved for 2 h in serum-free medium were treated with anti-CD36 mAb, its isotype control (1 μg/ml), or MOxLDL (at 50 μg/ml) for the indicated period of time. α-Tubulin contents on the same immunoblot are presented for control of loading. The molecular weight corresponding to the closest band of the ladder is indicated. (B) Macrophages infected with HIV-1 NLAD8 for 7 d were washed and pretreated for 30 min with medium supplemented or not with FA6-152 mAb or its isotype control at 2 μg/ml. Then medium with or without MOxLDL was added directly onto the cells to obtain the indicated final concentration of MOxLDL and to keep mAb final concentration at 1 μg/ml. Measure of the p24 Gag released during overnight treatment are presented. (C) Cell viability at the end of the experiment shown in B was measured with the CellTiter-Glo kit. (D) Macrophages at 7 d p.i. starved for 2 h in serum-free medium were treated with the anti-CD36 or with the isotype control mAb in complete medium (control), medium supplemented with lipoprotein deficient serum (LPDS), or serum-free medium (no serum). (E) Quantification of the p24 Gag released from HIV-1–infected macrophages treated overnight with the anti-CD36 antibody (FA6-152 at 2 μg/ml), its isotype control, or thrombospondin-1 (TSP-1) and type-I collagen (COL1) at the indicated concentrations. Representative experiments are shown. Except for D, which was performed twice, results were obtained at least three times with different donors. Data are presented as mean ± SEM of triplicates.

of p24 Gag released in the supernatant as compared with exposure to an isotype control antibody (Fig. 9 A). Conversely, and like in macrophages, the amounts of p24 Gag detected in the corresponding cell lysates increased (54% mean, $P \leq 0.001$ on three independent experiments) in anti-CD36–treated cells as compared with isotype-treated cells (Fig. 9 B). In contrast, viral release from HeLa cells lacking CD36 remained unaffected by both antibodies (Fig. 9, A and B). Immunoblot analysis of the Gag contents of the cell lysates confirmed the results obtained by Elisa (unpublished data). We conclude that the inhibitory effect of the anti-CD36 mAb on particle release can be reproduced in infected HeLa-CD36 cells.

Exposure of HIV-1–infected HeLa-CD36 cells to the anti-CD36 mAb induces large tethering of viral particles at the plasma membrane

To approach the mechanism of action of the anti-CD36 mAb, we analyzed HIV-1– Gag–iGFP-infected HeLa-CD36 cells exposed to the mAb for 48 h by confocal microscopy and observed the presence of large clusters of $Gag^{+}CD9^{+}$ material at the plasma membrane of cells exposed to the anti-CD36 mAb that were absent in isotype-treated cells (Fig. 9 C). Time-lapse microscopy of HeLa-CD36 cells infected with HIV-1 Gag-iGFP after addition of the anti-CD36 mAb allowed us to witness the formation of these large clusters at the plasma membrane (Video 2). Ultrastructural analysis of HIV-1–infected HeLa-CD36 cells confirmed the presence at the plasma membrane of these large clusters of virions upon anti-CD36 exposure, but not in the isotype-treated control cells (Fig. 9 D). Collectively these results suggest that the anti-CD36 exposure induces virions tethering at the site of viral assembly, i.e., in the VCCs of macrophages and at the plasma membrane of HeLa-CD36 cells.

The C-terminal tail of CD36 is not required for the anti-CD36–induced inhibition of HIV release

These results suggested that the anti-CD36 mAb effect did not rely on signal transduction via CD36. To further test the hypothesis, we took advantage of a previously published comparison of the cytoplasmic tail of CD36 with those of CD63, CD82, CD81, and CD9 (Primo et al., 2005). All these proteins are localized in the VCCs and present homologies (Fig. 9 E), as they possess a bulky/aromatic residue (position 4), a Cys (position 5), and a basic residue (position 9). This suggested that potential motifs of targeting to the VCCs

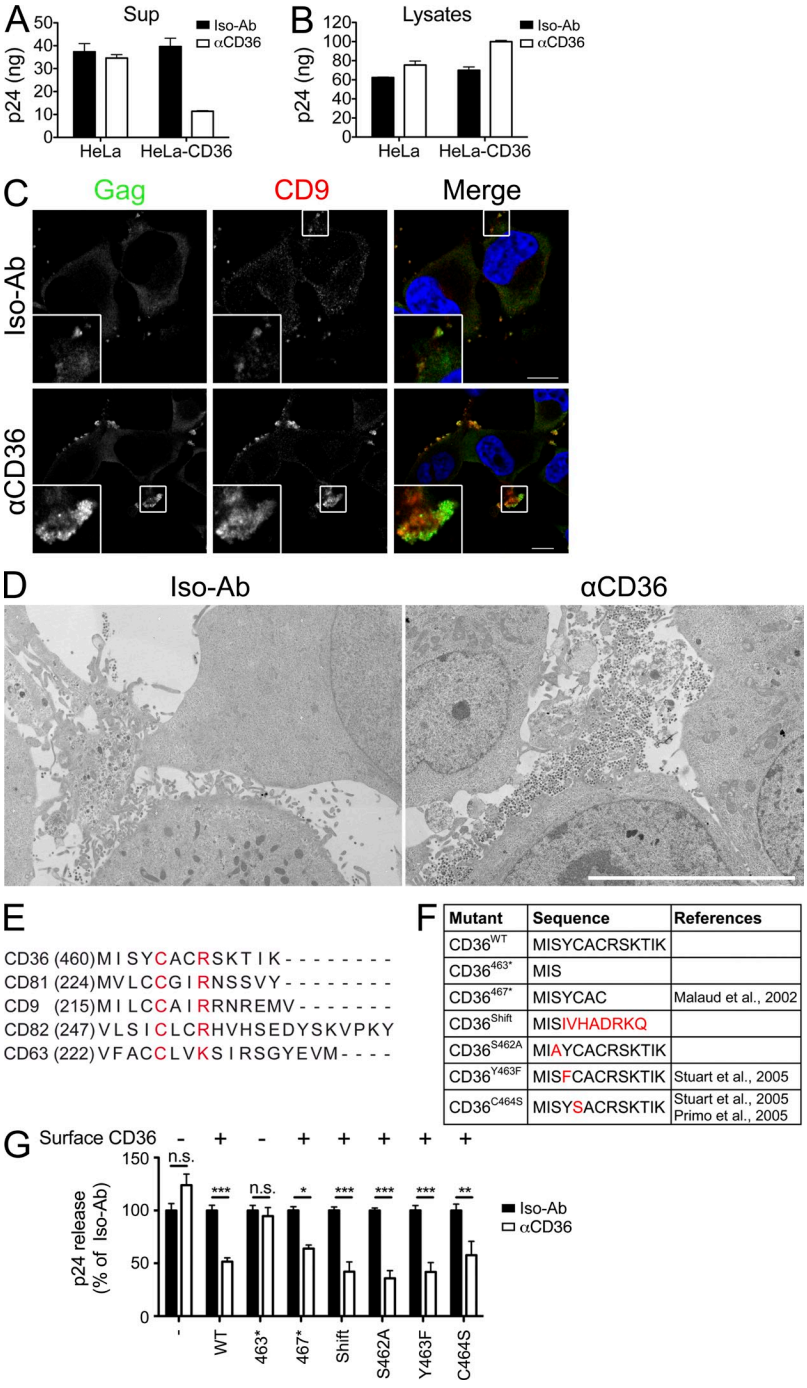

Mutant	Sequence	References
$CD36^{WT}$	MISYCACRSKTIK	
$CD36^{463*}$	MIS	
$CD36^{467*}$	MISYCAC	Malaud et al., 2002
$CD36^{Shift}$	MISIVHADRKQ	
$CD36^{S462A}$	MIAYCACRSKTIK	
$CD36^{Y463F}$	MISFCACRSKTIK	Stuart et al., 2005
$CD36^{C464S}$	MISYSACRSKTIK	Stuart et al., 2005 Primo et al., 2005

Figure 9. Anti-CD36 antibody treatment induces HIV-1 tethering at the plasma membrane of HeLa cells expressing CD36. Quantification of p24 Gag in the supernatant (A) and lysates (B) of HeLa and HeLa-CD36 cells treated with the FA6-152 mAb or with the IgG1 control overnight. A representative experiment is shown. The data shown are the means and SEM of triplicates. (C) Confocal sections of HeLa and HeLa-CD36 cells infected with HIV-1 Gag-iGFP, treated with the anti-CD36 mAb or its isotype control (Iso-Ab) for 48 h, and stained for CD9. Insets are enlargements of the boxed regions. Bars, 10 µm. Merge images include DAPI staining in blue. (D) Electron micrographs of HIV-1 NLAD8-infected HeLa-CD36 cells treated with FA6-152 mAb or its isotype control. Bar, 10 µm. (E) Multiple alignment illustrating the conserved residues present in the cytoplasmic tails of the proteins indicated. The figure was adapted from Primo et al. (2005). (F) Table showing the CD36 mutants produced with the corresponding changes in the C-tail sequence. The mutated amino acids are shown in red. The $CD36^{467*}$ and the $CD36^{Y463F}$ mutants are impaired for binding and capture of MOxLDL (Malaud et al., 2002) and for *Staphylococcus aureus* internalization (Stuart et al., 2005), respectively, whereas the $CD36^{C464S}$ mutant is impaired for *S. aureus* internalization (Stuart et al., 2005) and for loss of TSP-1–dependent VEGF-A165–induced migration (Primo et al., 2005). (G) Quantification of p24 Gag in the supernatant of HeLa cell lines stably expressing the indicated CD36 mutants, treated with the anti-CD36 mAb or its isotype control. CD36 cell surface expression was assessed by FACS (indicated by + or –). Data are presented as the means and SEM of three independent experiments performed on three different preparations of transduced cell lines, with the exception of the experiments with the 467* and C464S mutants which were independently repeated twice. Statistical analysis was performed by two-way ANOVA with Bonferroni's post hoc test (*, $P \leq 0.05$; **, $P \leq 0.01$; ***, $P \leq 0.001$).

may exist in the cytoplasmic tail of CD36 as well as other VCC proteins.

To identify key residues involved in the anti-CD36–mediated effect, we built a collection of CD36 mutants taking into account previous studies that have identified mutations altering several functions of CD36 (see Fig. 9 F and references in the legend). Each of the seven CD36 mutants, as well as the CD36 wild type, was cloned in a lentiviral vector that was used to establish stably expressing HeLa cells. Flow cytometry analysis revealed that all CD36 mutants were expressed at the cell surface, with the exception of the $CD36^{463*}$ mutant (unpublished data). Importantly, all the CD36 mutants expressed at the cell surface were sensitive to the inhibitory effect of the anti-CD36 mAb, like wild-type CD36 (Fig. 9 G). This includes point mutants of the conserved cysteine residue ($CD36^{C464S}$) and a mutant carrying in its coding sequence a frame shift leading to substitution and premature stop codon ($CD36^{shift}$). These data suggest that the effect of the anti-CD36 mAb does not require the integrity of the CD36 cytoplasmic tail, and thus, in all likelihood, signal transduction through CD36 does not occur.

CD36 mAb inhibits the release of a primary isolate and macrophage to T cell viral transmission

From a therapeutic perspective, we evaluated if our results could be extended to primary strains of HIV-1. Anti-CD36 mAb exposure of macrophages infected with the 132W primary isolate (Roesch et al., 2012) led to a strong reduction of the p24 Gag secreted in the supernatant (Fig. 10 A) and a concomitant increase of the cell-associated p24 Gag (Fig. 10 B) without affecting cell viability (Fig. 10 C). We conclude that anti-CD36 mAb exposure of macrophages infected with a primary HIV-1 isolate leads to the inhibition of viral secretion.

Cell-to-cell transmission is thought to be much more efficient than cell-free virus infection (Chen et al., 2007; Sourisseau et al., 2007). To test the effect of the anti-CD36 mAb on macrophage–to–T cell transmission, primary activated CD4$^+$ T cells were added to HIV-1–infected macrophages together with the anti-CD36 mAb or its isotype control. After 24 h, AZT was added to stop new infections. The culture was left for an additional 24 h to allow Gag to accumulate into infected T cells, the proportion of which was measured by intracellular staining. As a positive control, we used anti–ICAM-1 mAb, which is known to inhibit cell-to-cell transfer of HIV-1 (Jolly et al., 2007; Wang et al., 2009). Importantly, the anti-CD36 mAb exposure like the anti–ICAM-1 mAb but not the isotype control led to a strong reduction of the fraction of T cells that became infected (Fig. 10 D). Therefore, exposure to anti-CD36 mAb can inhibit macrophage–to–T cell transmission of HIV-1.

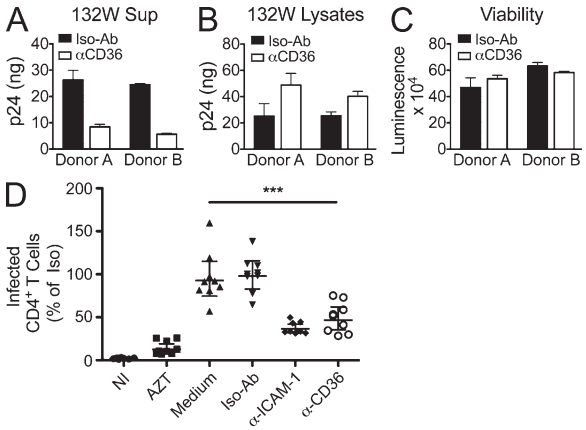

Figure 10. Effect of anti-CD36 antibody exposure on macrophages infected with a primary isolate and on macrophage–to–T cell transmission. (A and B) Macrophages from two donors were infected with the primary HIV-1 isolate 132W and treated at day 7 p.i. with anti-CD36 mAb or isotype control as in Fig. 5 (A–C). p24 Gag contents were measured in culture supernatant (A) and in corresponding cell lysates (B). (C) Cell viability measured at the end of the experiment with the CellTiter-Glo kit. Data are presented as mean ± SEM of triplicates. (D) Macrophage–to–T cell HIV-1–transmission after co-culture of heterologous, activated primary CD4$^+$ T cells with HIV-1–infected macrophages in the indicated conditions. Percentage of infected CD4$^+$ T cells after co-culture was measured by intracellular FACS staining of Gag. Data presented were obtained from three independent experiments performed on cells from three different donors and are shown as Geo Mean with 95% CI. One-way ANOVA with Tukey's multiple comparison test was used as statistic test (***, $P \leq 0.001$).

DISCUSSION

Although still incomplete, current knowledge points to macrophages as key players in the course of HIV-1 infection and as a potential reservoir from which infection can rebound upon arrest of highly active antiretroviral therapy. It is thus crucial to decipher the life cycle of HIV-1 within macrophages, especially the late phases that remain poorly understood. In macrophages, HIV-1 assembly occurs in internal compartments, often referred to as VCCs, that probably originate from the plasma membrane (Deneka et al., 2007; Welsch et al., 2007). Our study reveals that HIV-1 hijacks preexisting CD36$^+$ compartments for viral assembly and storage, and that CD36 expression is required for completion of the viral cycle. We also show that exposure to antibodies specific for CD36 induces the intracellular retention of the virions in infected macrophages and thus inhibits their release and transmission to T cells.

Our results showing a relationship between the VCC and preexisting compartments present in uninfected macrophages shed new light on the mysterious nature of the VCC (Tan and Sattentau, 2013). We show, both in uninfected and in HIV-infected macrophages, the presence of CD36$^+$CD9$^+$ CD81$^+$Lamp1$^-$ compartments that can be connected to the surface. Furthermore, we show by time-lapse microscopy, for the first time to our knowledge, that internal CD36$^+$ compartments preexist in macrophages and represent the site where newly synthesized cytosolic Gag accumulates, converting these compartments into VCCs with time. These data are consistent with previous studies (Deneka et al., 2007; Welsch et al., 2011; Chu et al., 2012a; Pelchen-Matthews et al., 2012) and indicate together that HIV-1 takes advantage of the existence of these macrophage-specific compartments. This feature of the macrophage may explain, at least in part, why VCCs are exclusive to macrophages.

How the viral precursor p55 Gag is recruited to preexisting CD36$^+$ compartments remains unclear but may be linked to the capacity of both proteins to preferentially associate with membrane rafts (Nguyen and Hildreth, 2000; Ono and Freed, 2001; Zeng et al., 2003; Wolf et al., 2007). Although we did not find any evidence for a direct CD36–Gag interaction, it may occur indirectly, for instance through CD9. Indeed, we observed in uninfected macrophages an extensive co-distribution of CD36 and CD9. Moreover, CD36 has been shown to interact with CD9 (Miao et al., 2001; Huang et al., 2011; Kazerounian et al., 2011; Heit et al., 2013) and p55 Gag to sequester CD9 in plasma membrane rafts (Krementsov et al., 2010).

In macrophages, CD36 motion is subjected to linear confinement due to cytoskeleton constraints thereby promoting receptor encounters and clustering (Jaqaman et al., 2011). Interestingly, ligand internalization via CD36 occurs through the formation of multimolecular complexes together with β1 or β2 integrins, and CD9 and/or CD81 (Heit et al., 2013), which are components of the VCC (Deneka et al., 2007;

Pelchen-Matthews et al., 2012) and of the membrane of HIV-1 particles produced by macrophages (Chertova et al., 2006). The tetraspanins CD9 and CD81 are present in membrane microdomains often referred to as TEM (tetraspanin-enriched microdomains) that are distinct from lipid raft microdomains (Nydegger et al., 2006). Importantly, through its oligomerization, p55 Gag promotes the coalescence of TEM and lipid rafts in HeLa cells. Therefore, from all these studies, we can hypothesize that Gag oligomerization at the cytosolic face of $CD36^+$ membranes can be instrumental in the recruitment and concentration of TEMs together with lipid rafts, bringing together several tetraspanins through a network of membrane interactions. Such recruitment may favor the formation of platforms conducive to viral budding. Future work will aim at elucidating the precise role of CD36 in the HIV-1 cycle in macrophages.

Another major finding of the present study is that exposure of infected macrophages to CD36-specific antibodies inhibits viral release by inducing their intracellular retention. The viral content within the anti-CD36 antibody-treated cells was greater than in cells treated with an isotype control antibody and the VCCs were larger. Importantly, this corresponded to a reduced ability of the macrophages to transfer virus to primary T cells. In addition, this inhibitory effect appears to be virus-specific, as the viral production of influenza-infected macrophages remained unaffected by their exposure to the anti-CD36 mAb (unpublished data).

The anti-CD36 antibody effect on HIV-1 release was exclusive, as antibodies specific for other scavenger receptors or other VCC markers such as CD81, ICAM-1, and CD9 did not affect HIV-1 release. Antibodies specific for CD36, CD81, and ICAM-1 were internalized into most of the Gag^+ compartments after 2 h of incubation at 37°C. In an experimental system similar to ours (3 h at 37°C), anti-CD63 antibodies accessed VCCs in HIV-1–infected macrophages (Deneka et al., 2007). Others (Chu et al., 2012b) and us have found that antibodies specific to CD9, CD63, CD81, and ICAM-1 do not access VCCs at 4°C or in fixed nonpermeabilized cells. It is therefore likely that, in HIV-1–infected macrophages, specific antibodies can be internalized into VCCs through an active mechanism that does not take place at 4°C but requires time to become detectable by immunofluorescence (mAbs were only weakly detected in VCCs 1 h after incubation in our experiments and in another study [Koppensteiner et al., 2012]). However, although other antibodies could be taken up into the VCC, only exposure to anti-CD36 antibodies led to the intracellular retention of virions.

The mechanism of the antibody-mediated inhibition of HIV-1 release does not seem to rely on signaling through CD36. Indeed, we show that the inhibitory effect of the mAb on HIV-1 release can be reproduced in HeLa cells transduced with CD36 wt, but also with CD36 deleted from (or substituted in) most of its cytoplasmic tail. This includes CD36 mutated in key residues of the cytoplasmic tail required for CD36 signaling (Fig. 9 F, references). We also show that endogenous ligands of CD36, MOxLDL, TSP1, and COL1 do not inhibit viral particle release by infected macrophages while they induce signaling.

Similarly, Fc receptor signaling does not seem to be involved in the CD36-specific mAb inhibitory effect on viral release. Indeed, HeLa-CD36 cells, which do not express FcR, are susceptible to the antibody-mediated inhibition. In addition, all our experiments have been performed in parallel using isotype controls, which did not affect viral release. Similarly, antibodies specific for ICAM-1, CD81, and CD9 that are able to bind viral particles, as well as engage FcRs, had no effect on viral release. (Of note, the anti–ICAM-1 mAb is the same isotype as the anti-CD36 mAb.) Finally, blockage of FcR binding and signaling using a commercial FcR antagonist had no effect on the anti-CD36 mAb-mediated inhibition of particle release by macrophages.

Different hypotheses can be evoked to explain the antibody-induced retention, including the clustering of the virions within the VCC lumen through mAb binding to CD36 on the viral membrane and on the limiting membrane of the VCC. Immuno-EM analysis of HIV-1–infected macrophages exposed to anti-CD36 mAb reveals that the inhibitory mAb is associated with virions present within the lumen of the VCCs. Similar experiments performed with HIV-1–infected HeLa-CD36 cells revealed clustering of the virions at their assembly site, i.e., at the plasma membrane. In all likelihood, exogenously added anti-CD36 mAb access the VCCs of infected macrophages, where they retain virions. Moreover, our data are compatible with the idea that the antibody effect could take place without affecting the virions themselves, at least in the short term, because free virions remain equally infectious in the presence of the anti-CD36 antibody.

Further supporting the clustering effect of the mAb, the anti-CD36 mAb FA6-152, but not its Fab fragment, mediates the inhibition of virion release, suggesting that bivalency of the mAb is required. In contrast to FA6-152, SMΦ mAb does not inhibit HIV-1 release. Both mAbs are specific for the same CD36 region (155–183; Daviet et al., 1995), but their epitopes have not been precisely defined and can be different. The fact that SMΦ is an IgM and FA6-152 an IgG1 supports the idea of a clustering induced by the bivalent ligand (FA6-152) and not by multivalent ligands like MOxLDL or SMΦ. It can be proposed that the density of CD36 on the virion and VCC membranes, and the valence and affinity of the mAbs are critical for the clustering effect. However, more complex mechanisms cannot be excluded. For instance, the tetherin/BST2 protein has been recently shown to be important for HIV-1 viral cycle in macrophages, possibly by mediating retention of the virions in the VCCs (Chu et al., 2012a). In our system, the anti-CD36 antibody exposure did not modify the level of expression of tetherin/BST2 even after 2 d of treatment (unpublished data). However, this does not rule out a possible contribution of tetherin/BST2 in the observed retention of virions within VCCs.

Our data show that the anti-CD36 antibody-induced retention of virions into VCCs results in a powerful inhibition of virus release and of macrophage to T cell transmission of

HIV-1. Given that HIV-1 is a fragile virus, the increased intracellular retention induced by repeated exposures could lead, in time, to a strong reduction of the infectious capacity of the intracellular stocks of virions. In addition, we recently showed that the amounts of virus released by infected macrophages and their infectious capacity both decrease with time p.i. (Gaudin et al., 2013). Therefore, it may be possible to use anti-CD36 mAbs to complement existing antiviral treatments to target viral reservoirs within macrophages.

MATERIALS AND METHODS

Antibodies and reagents. Goat polyclonal antibody anti-p24 Gag, mouse mAbs specific for human CD81 (clone TS81), CD68 (clone KP1), and SRA1 (clone 7H1G1), and rabbit antibodies specific for human LDLR (clone EP1553Y) were purchased from Abcam. We also used rabbit polyclonal antibody anti–SR-B1 (Novus Biologicals), mAbs specific for CD9 (MEM-61; Immunotools), ICAM-1 (clone HA58; BD), and CD36 (clones CLB-IVC7 and TR9 from Immunotools and Acris Antibodies, and clone FA6-152 from STEMCELL Technologies), unlabeled isotype controls (BD), and secondary antibodies conjugated with Alexa Fluor 488 or 647 (Life Technologies), Cy3, or Cy5 (Jackson ImmunoResearch Laboratories). FITC- and PE-labeled isotype controls, as well as anti-p24 Gag (KC57-FITC or KC-57 RD1), were purchased from Beckman Coulter, whereas FITC- and PE-labeled anti-CD36 (CLB-IVC7 and TR9) were purchased from Immunotools. Alexa Fluor 647–coupled anti-CD36 (clone SMΦ), its isotype control, and rabbit polyclonal anti-CD9 antibodies (H-110) were purchased from Santa Cruz Biotechnology, Inc. Human antibodies specific for EGFP and rabbit antibodies anti–α-tubulin were given by A. El Marjou (Institut Curie, Paris, France). The phospho-SAPK/JNK (Thr183/Tyr185; 81E11) rabbit mAb from Cell Signaling Technology was used. Antibodies specific for p17 Gag, as well as p55 Gag (National Institutes of Health [NIH] AIDS reagents 4811 from P. Spearman, Children's Healthcare of Atlanta and Emory University School of Medicine, Atlanta, GA), and HIV immunoglobulins (used at 0.37 mg/ml in the infectivity assay on TZM-bl cells) were obtained through the NIH AIDS Research and Reference Reagent Program, Division of AIDS, National Institute of Allergy and Infectious Diseases, NIH. Fab fragments were produced using the Mouse IgG1 Fab and F(ab′)2 Preparation kit (Thermo Fisher Scientific). The human FcR Blocking Reagent (Miltenyi Biotec) was tested by FACS for its capacity to stain the plasma membrane of primary macrophages and was used according to the manufacturer's guidelines. Each tube of MOxLDL (Kalen Biomedical) was used for a single experiment within 1 wk from the shipment date to avoid oxidation. TSP-1 was purchased from EMD Millipore, whereas collagen type I was purchased from Sigma-Aldrich. We also used dextran coupled to Alexa Fluor 647 10,000 MW (Molecular Probes), IL2 (eBioscience), PHA-L (Sigma-Aldrich), AZT (Sigma-Aldrich), and rhM-CSF (Immunotools) dissolved in ultrapure water (25 µg/ml stock).

Plasmids. pVSV-G (BD), pEGFP N1 (Takara Bio Inc.), and psPax2 (Addgene number 12260) plasmids were used. pHIV-1 Gag-iGFP, which carries an R5-tropic envelope with the V3-loop V92th014.12 (Koppensteiner et al., 2012), and pHIV-1 Gag-iGFPΔEnv were provided by M. Schindler (Institute of Virology, Helmholtz Zentrum Munich, Munich, Germany). The pHIV-1 Gag-iCherryΔEnv was obtained by subcloning the region from NarI to BamHI from the pHIV-1 Gag-iGFP into pUNO-mcs vector (InvivoGen). Then, the GFP was replaced with the mCherry sequence amplified with the primers mCherry_F_MluI (5′-TGTACAAACGCGTGTGAGCAAGGGCGAGGAG-3′) and mCherry_R_XbaI (5′-TTGGCTTCTAGACTTGTACAGCTCGTCCATGC-3′) using the restriction sites XbaI and MluI. The fragment obtained, containing the mCherry in place of the GFP, was then recloned in the pHIV-1 Gag-iGFPΔEnv backbone using BssHII and SpeI. To build the lentiviral vector pEXP DH1 CD36, the CD36 cDNA from the pENT221 CD36 (DNASU reference HsCD00045106) was cloned with Gateway technology (Life Technologies) into a pDEST DH1, which is a modified version of pCDH1 (System Bioscience) in which the MCS has been replaced by a Gateway cassette. To construct CD36-GFP, pENT221 CD36 was used as a template to amplify the CD36 cDNA with the primers CD36 N1 forward (5′-ACCGCGGGCCCGGGATATGGGCTGTGACCGGAACTG-3′) and CD36 N1 reverse (5′-CATGGTGGCGACCGGTGGTTTTATTGTTTTCGATCTGCATGCAC-3′). The PCR product was then cloned into the pEGFP N1 using the restriction sites XmaI and AgeI. The resulting cDNAs CD36-GFP were cloned with Gateway technology back into pDONR201and then to a pDEST DH1. CD36 mutants were produced with the QuikChange II Site-Directed Mutagenesis kit (Agilent Technologies) using the pEXP DH1 CD36 as template. Primers were designed with the QuikChange Primer Design Program (Agilent Technologies).

Primary cells and cell lines. Purification, differentiation, and culture of monocytes and macrophages, as well as culture of the cell lines Ghost, HEK293T (CRL-11268; ATCC), and TZM-bl, were performed as previously described (Gaudin et al., 2012). HeLa-CD36 cells were produced by lentiviral transduction of the CD36 gene. Puromycin selection (at 4 µg/ml; InvivoGen) was performed to obtain a pure population of transduced cells. HeLa cells, as well as HeLa cells expressing the different CD36 mutants, were cultured in DMEM with GlutaMAX completed with 10% FCS (Gibco) and 1% penicillin-streptomycin (Gibco).

Virus preparations and infections. The following virus strains have been produced for the present study: NL(AD8) (NLAD8), NL4-3, HIV-1 Gag-iGFP, HIV-1 Gag-iGFP ΔEnv, and HIV-1 Gag-iCherry ΔEnv. Viruses were produced by cotransfection of the appropriate proviral cDNA, and the pVSV-G plasmid into 293T cells using GeneJuice (EMD Millipore). Supernatants were harvested 72 h after transfection, filtered, and stored at −80°C. Virus preparations were titrated by infecting the Ghost reporter cell line and infectivity was measured 24 h p.i. by flow cytometry as previously described (Mörner et al., 1999). For infection experiments, macrophages were infected at a multiplicity of infection (MOI) of 0.2 and kept in culture for indicated times. HeLa cells were infected at MOI 0.5. The 132W primary isolate (used at 10 ng p24 Gag for 10^5 macrophages) was a gift of O. Schwartz (Pasteur Institute, Paris, France). Lentiviral vectors have been produced for pEXP DH1 CD36, pEXP DH1 CD36-GFP, and for all the CD36 mutants used in Fig. 9. Transducing lentiviruses were produced with the same protocol described for the HIV-1 viral strains with the addition of the packaging psPax2 plasmid. SIV-VLP were produced and used as previously described (Goujon et al., 2008; Manel et al., 2010).

Viral production and infectivity assays. Measure of HIV-1 p24 Gag was performed using the Innotest HIV Ag mAb Screening kit (Ingen). Cell viability was evaluated using the CellTiter-Glo (Promega). For infectivity assays, virion-containing supernatants were normalized for equal amounts of p24 Gag (final concentration of 10 ng/ml) and infectious titers were determined using TZM-bl indicator cells as previously described (Gaudin et al., 2012).

RNA interference. Luciferase-specific, Tsg101-specific (Gaudin et al., 2012), and CD36-specific (Hs_CD36_1/6/7; QIAGEN) siRNA were used. siRNAs (100 nM final) were diluted in 250 µl OptiMEM (Gibco) mixed with 5 µl INTERFERin (Polyplus) and left at room temperature for 15 min. Complexes were added drop-wise onto the macrophage cultures. Cells were assayed 3 d later. Knockdown efficiency was checked by flow cytometry.

Immunofluorescence, image quantification, immuno-EM, and live imaging. For immunofluorescence, cells were stained and imaged as previously described (Gaudin et al., 2012). For antibody feeding assay (Fig. 4; and Fig. 6, A and B), cells were precooled at 4°C for 20 min before replacing the medium with ice-cold medium containing the antibody of interest or its isotype control. Cells were kept at 4°C or moved to 37°C for 2 h depending on the condition before fixation and staining. Confocal images were collected as snapshot or 3D stacks with a focal step size of 0.5 µm. NIS Element, MetaMorph, and ImageJ software were used for image processing. No filter or background subtraction was used. Live imaging was performed using a

Nikon Biostation IM-Q using a 20× objective. To test the connection of VCCs to the plasma membrane (Fig. 2), cells were imaged with a microscope (Ti Inverted; Nikon) fitted with a video-rate confocal system consisting of a spinning disk confocal head (Yokogawa). HIV-1–infected macrophage samples were prepared for EM as previously described (Gaudin et al., 2012).

Image quantification For quantification of the Pearson's coefficient, 3D stacks (z = 0.5 µm) of infected macrophages were acquired with a confocal system (A1R; Nikon) and analyzed with the NIS Element Ar software. For each cell, a background of 100 for each channel was subtracted and plans containing no signal were discarded. Then the Pearson's coefficient of each plan of the stack was calculated, generating mean Pearson's coefficient per cell.

To quantify the total volume of VCCs per cell, the total intensity of Gag into VCCs per cell, and the number of VCCs per cell, confocal plans with a z-step of 0.25 µm were acquired for >134 cells per condition. VCCs were 3D-reconstructed and analyzed in a blind manner using IMARIS 7.2.3 software. Gag fluorescence intensity corresponding to the VCCs was detected, smoothed at 0.15 µm, and a background subtraction was applied based on largest sphere diameter (0.8 µm) criteria. Automatic segmentation was performed based on a region growing estimated diameter of 0.8 µm. Then, objects were filtered to take into account only VCCs >0.050 μm^3. Automated statistical analysis was run to extract the different parameters for each condition.

Immunoblotting. Analyses were performed as previously described (Gaudin et al., 2012), except for pJNK assay where lysis buffer was supplemented with 5 mM NaF and 1 mM β-glycerophosphate.

CD36 mAb blocking assay. Infected macrophages were washed extensively and exposed to the various antibodies and isotype controls at 37°C for various periods of time. All antibodies were dialyzed in PBS 1× and filtered before use. Content in p24 Gag in the supernatant and in cells lysed in the CellTiter-Glo buffer for 2 h at 4°C was determined by Elisa.

Macrophage–to–T cell HIV transmission assay. Macrophages (10^5 cells/well) were infected with VSV-G–pseudotyped NL4-3 at MOI 1.5, washed extensively 6 d later, and received 1.5×10^5 $CD4^+$ T lymphocytes/well. These $CD4^+$ T lymphocytes were purified by negative selection (Miltenyi Biotec) from heterologous PBMCs that had been activated 48 h before in RPMI, 10% FCS, 2.5 µg/ml PHA-L, and 30 U/ml IL2. 25 µM AZT was added at 0 h (as a negative control) or 24 h after the beginning of the co-cultures. At 48 h, $CD4^+$ T cells were collected, washed, fixed with 1% PFA, permeabilized, stained for Gag with KC57-FITC mAb, and analyzed by flow cytometry in a flow cytometer (Accuri C6; BD).

Online supplemental material. Video 1 corresponds to Fig. 3. Video 2 corresponds to Fig. 9.

The authors greatly acknowledge the Nikon Imaging Center@Institut Curie-Centre National de la Recherche Scientifique, as well as S. Amigorena, N. Manel, and A.-M. Lennon-Dumenil for discussions. We thank Aditi Varthaman for editing the English version of the manuscript.

Work was supported by grants from Agence Nationale de Recherche contre le SIDA (ANRS) and Ensemble contre le SIDA (Sidaction) to P. Benaroch and fellowships to R. Gaudin (ANRS), S. Berre (Curie Institute), M. Desdouits (ANRS), and B. Cunha de Alencar (Fondation pour la Recherche Médicale).

The authors declare no competing financial interests.

Submitted: 18 March 2013
Accepted: 1 October 2013

REFERENCES

Areschoug, T., and S. Gordon. 2009. Scavenger receptors: role in innate immunity and microbial pathogenesis. *Cell. Microbiol.* 11:1160–1169. http://dx.doi.org/10.1111/j.1462-5822.2009.01326.x

Asch, A.S., J. Barnwell, R.L. Silverstein, and R.L. Nachman. 1987. Isolation of the thrombospondin membrane receptor. *J. Clin. Invest.* 79:1054–1061. http://dx.doi.org/10.1172/JCI112918

Benaroch, P., E. Billard, R. Gaudin, M. Schindler, and M. Jouve. 2010. HIV-1 assembly in macrophages. *Retrovirology*. 7:29. http://dx.doi.org/10.1186/1742-4690-7-29

Bennett, A.E., K. Narayan, D. Shi, L.M. Hartnell, K. Gousset, H. He, B.C. Lowekamp, T.S. Yoo, D. Bliss, E.O. Freed, and S. Subramaniam. 2009. Ion-abrasion scanning electron microscopy reveals surface-connected tubular conduits in HIV-infected macrophages. *PLoS Pathog.* 5:e1000591. http://dx.doi.org/10.1371/journal.ppat.1000591

Chen, P., W. Hübner, M.A. Spinelli, and B.K. Chen. 2007. Predominant mode of human immunodeficiency virus transfer between T cells is mediated by sustained Env-dependent neutralization-resistant virological synapses. *J. Virol.* 81:12582–12595. http://dx.doi.org/10.1128/JVI.00381-07

Chertova, E., O. Chertov, L.V. Coren, J.D. Roser, C.M. Trubey, J.W. Bess Jr., R.C. Sowder II, E. Barsov, B.L. Hood, R.J. Fisher, et al. 2006. Proteomic and biochemical analysis of purified human immunodeficiency virus type 1 produced from infected monocyte-derived macrophages. *J. Virol.* 80:9039–9052. http://dx.doi.org/10.1128/JVI.01013-06

Chu, H., J.-J. Wang, M. Qi, J.-J. Yoon, X. Chen, X. Wen, J. Hammonds, L. Ding, and P. Spearman. 2012a. Tetherin/BST-2 is essential for the formation of the intracellular virus-containing compartment in HIV-infected macrophages. *Cell Host Microbe*. 12:360–372. http://dx.doi.org/10.1016/j.chom.2012.07.011

Chu, H., J.-J. Wang, M. Qi, J.-J. Yoon, X. Wen, X. Chen, L. Ding, and P. Spearman. 2012b. The intracellular virus-containing compartments in primary human macrophages are largely inaccessible to antibodies and small molecules. *PLoS ONE*. 7:e35297. http://dx.doi.org/10.1371/journal.pone.0035297

Collins, R.F., N. Touret, H. Kuwata, N.N. Tandon, S. Grinstein, and W.S. Trimble. 2009. Uptake of oxidized low density lipoprotein by CD36 occurs by an actin-dependent pathway distinct from macropinocytosis. *J. Biol. Chem.* 284:30288–30297. http://dx.doi.org/10.1074/jbc.M109.045104

Daviet, L., R. Buckland, M.D. Puente Navazo, and J.L. McGregor. 1995. Identification of an immunodominant functional domain on human CD36 antigen using human-mouse chimaeric proteins and homologue-replacement mutagenesis. *Biochem. J.* 305:221–224.

Deneka, M., A. Pelchen-Matthews, R. Byland, E. Ruiz-Mateos, and M. Marsh. 2007. In macrophages, HIV-1 assembles into an intracellular plasma membrane domain containing the tetraspanins CD81, CD9, and CD53. *J. Cell Biol.* 177:329–341. http://dx.doi.org/10.1083/jcb.200609050

Endemann, G., L.W. Stanton, K.S. Madden, C.M. Bryant, R.T. White, and A.A. Protter. 1993. CD36 is a receptor for oxidized low density lipoprotein. *J. Biol. Chem.* 268:11811–11816.

Garrus, J.E., U.K. von Schwedler, O.W. Pornillos, S.G. Morham, K.H. Zavitz, H.E. Wang, D.A. Wettstein, K.M. Stray, M. Côté, R.L. Rich, et al. 2001. Tsg101 and the vacuolar protein sorting pathway are essential for HIV-1 budding. *Cell*. 107:55–65. http://dx.doi.org/10.1016/S0092-8674(01)00506-2

Gaudin, R., B.C. de Alencar, M. Jouve, S. Bèrre, E. Le Bouder, M. Schindler, A. Varthaman, F.-X. Gobert, and P. Benaroch. 2012. Critical role for the kinesin KIF3A in the HIV life cycle in primary human macrophages. *J. Cell Biol.* 199:467–479. http://dx.doi.org/10.1083/jcb.201201144

Gaudin, R., S. Berre, B. Cunha de Alencar, J. Decalf, M. Schindler, F.-X. Gobert, M. Jouve, and P. Benaroch. 2013. Dynamics of HIV-containing compartments in macrophages reveal sequestration of virions and transient surface connections. *PLoS ONE*. 8:e69450. http://dx.doi.org/10.1371/journal.pone.0069450

Goujon, C., V. Arfi, T. Pertel, J. Luban, J. Lienard, D. Rigal, J.-L. Darlix, and A. Cimarelli. 2008. Characterization of simian immunodeficiency virus SIVSM/human immunodeficiency virus type 2 Vpx function in human myeloid cells. *J. Virol.* 82:12335–12345. http://dx.doi.org/10.1128/JVI.01181-08

Gyorkey, F., J.L. Melnick, J.G. Sinkovics, and P. Gyorkey. 1985. Retrovirus resembling HTLV in macrophages of patients with AIDS. *Lancet*. 1:106. http://dx.doi.org/10.1016/S0140-6736(85)91995-6

Heit, B., H. Kim, G. Cosío, D. Castaño, R. Collins, C.A. Lowell, K.C. Kain, W.S. Trimble, and S. Grinstein. 2013. Multimolecular signaling complexes enable

Syk-mediated signaling of CD36 internalization. *Dev. Cell*. 24:372–383. http://dx.doi.org/10.1016/j.devcel.2013.01.007

Hoebe, K., P. Georgel, S. Rutschmann, X. Du, S. Mudd, K. Crozat, S. Sovath, L. Shamel, T. Hartung, U. Zähringer, and B. Beutler. 2005. CD36 is a sensor of diacylglycerides. *Nature*. 433:523–527. http://dx.doi.org/10.1038/nature03253

Huang, W., M. Febbraio, and R.L. Silverstein. 2011. CD9 tetraspanin interacts with CD36 on the surface of macrophages: a possible regulatory influence on uptake of oxidized low density lipoprotein. *PLoS ONE*. 6:e29092. http://dx.doi.org/10.1371/journal.pone.0029092

Jaqaman, K., H. Kuwata, N. Touret, R. Collins, W.S. Trimble, G. Danuser, and S. Grinstein. 2011. Cytoskeletal control of CD36 diffusion promotes its receptor and signaling function. *Cell*. 146:593–606. http://dx.doi.org/10.1016/j.cell.2011.06.049

Jarry, A., A. Cortez, E. René, F. Muzeau, and N. Brousse. 1990. Infected cells and immune cells in the gastrointestinal tract of AIDS patients. An immunohistochemical study of 127 cases. *Histopathology*. 16:133–140. http://dx.doi.org/10.1111/j.1365-2559.1990.tb01081.x

Jolly, C., I. Mitar, and Q.J. Sattentau. 2007. Adhesion molecule interactions facilitate human immunodeficiency virus type 1-induced virological synapse formation between T cells. *J. Virol*. 81:13916–13921. http://dx.doi.org/10.1128/JVI.01585-07

Jouve, M., N. Sol-Foulon, S. Watson, O. Schwartz, and P. Benaroch. 2007. HIV-1 buds and accumulates in "nonacidic" endosomes of macrophages. *Cell Host Microbe*. 2:85–95. http://dx.doi.org/10.1016/j.chom.2007.06.011

Kazerounian, S., M. Duquette, M.A. Reyes, J.T. Lawler, K. Song, C. Perruzzi, L. Primo, R. Khosravi-Far, F. Bussolino, I. Rabinovitz, and J. Lawler. 2011. Priming of the vascular endothelial growth factor signaling pathway by thrombospondin-1, CD36, and spleen tyrosine kinase. *Blood*. 117:4658–4666. http://dx.doi.org/10.1182/blood-2010-09-305284

Koenig, S., H.E. Gendelman, J.M. Orenstein, M.C. Dal Canto, G.H. Pezeshkpour, M. Yungbluth, F. Janotta, A. Aksamit, M.A. Martin, and A.S. Fauci. 1986. Detection of AIDS virus in macrophages in brain tissue from AIDS patients with encephalopathy. *Science*. 233:1089–1093. http://dx.doi.org/10.1126/science.3016903

Koppensteiner, H., C. Banning, C. Schneider, H. Hohenberg, and M. Schindler. 2012. Macrophage internal HIV-1 is protected from neutralizing antibodies. *J. Virol*. 86:2826–2836. http://dx.doi.org/10.1128/JVI.05915-11

Krementsov, D.N., P. Rassam, E. Margeat, N.H. Roy, J. Schneider-Schaulies, P.-E. Milhiet, and M. Thali. 2010. HIV-1 assembly differentially alters dynamics and partitioning of tetraspanins and raft components. *Traffic*. 11:1401–1414. http://dx.doi.org/10.1111/j.1600-0854.2010.01111.x

Kuniyasu, A., N. Ohgami, S. Hayashi, A. Miyazaki, S. Horiuchi, and H. Nakayama. 2003. CD36-mediated endocytic uptake of advanced glycation end products (AGE) in mouse 3T3-L1 and human subcutaneous adipocytes. *FEBS Lett*. 537:85–90. http://dx.doi.org/10.1016/S0014-5793(03)00096-6

Kunjathoor, V.V., M. Febbraio, E.A. Podrez, K.J. Moore, L. Andersson, S. Koehn, J.S. Rhee, R. Silverstein, H.F. Hoff, and M.W. Freeman. 2002. Scavenger receptors class A-I/II and CD36 are the principal receptors responsible for the uptake of modified low density lipoprotein leading to lipid loading in macrophages. *J. Biol. Chem*. 277:49982–49988. http://dx.doi.org/10.1074/jbc.M209649200

Malaud, E., D. Hourton, L.M. Giroux, E. Ninio, R. Buckland, and J.L. McGregor. 2002. The terminal six amino-acids of the carboxy cytoplasmic tail of CD36 contain a functional domain implicated in the binding and capture of oxidized low-density lipoprotein. *Biochem. J.* 364:507–515. http://dx.doi.org/10.1042/BJ20011373

Manel, N., B. Hogstad, Y. Wang, D.E. Levy, D. Unutmaz, and D.R. Littman. 2010. A cryptic sensor for HIV-1 activates antiviral innate immunity in dendritic cells. *Nature*. 467:214–217. http://dx.doi.org/10.1038/nature09337

Marsh, M., K. Theusner, and A. Pelchen-Matthews. 2009. HIV assembly and budding in macrophages. *Biochem. Soc. Trans.* 37:185–189. http://dx.doi.org/10.1042/BST0370185

Matsumoto, K., K. Hirano, S. Nozaki, A. Takamoto, M. Nishida, Y. Nakagawa-Toyama, M.Y. Janabi, T. Ohya, S. Yamashita, and Y. Matsuzawa. 2000. Expression of macrophage (Mphi) scavenger receptor, CD36, in cultured human aortic smooth muscle cells in association with expression of peroxisome proliferator activated receptor-gamma, which regulates gain of Mphi-like phenotype in vitro, and its implication in atherogenesis. *Arterioscler. Thromb. Vasc. Biol*. 20:1027–1032. http://dx.doi.org/10.1161/01.ATV.20.4.1027

Miao, W.-M., E. Vasile, W.S. Lane, and J. Lawler. 2001. CD36 associates with CD9 and integrins on human blood platelets. *Blood*. 97:1689–1696. http://dx.doi.org/10.1182/blood.V97.6.1689

Mörner, A., A. Björndal, J. Albert, V.N. Kewalramani, D.R. Littman, R. Inoue, R. Thorstensson, E.M. Fenyö, and E. Björling. 1999. Primary human immunodeficiency virus type 2 (HIV-2) isolates, like HIV-1 isolates, frequently use CCR5 but show promiscuity in coreceptor usage. *J. Virol*. 73:2343–2349.

Nguyen, D.H., and J.E.K. Hildreth. 2000. Evidence for budding of human immunodeficiency virus type 1 selectively from glycolipid-enriched membrane lipid rafts. *J. Virol*. 74:3264–3272. http://dx.doi.org/10.1128/JVI.74.7.3264-3272.2000

Nozaki, S., H. Kashiwagi, S. Yamashita, T. Nakagawa, B. Kostner, Y. Tomiyama, A. Nakata, M. Ishigami, J. Miyagawa, K. Kameda-Takemura, et al. 1995. Reduced uptake of oxidized low density lipoproteins in monocyte-derived macrophages from CD36-deficient subjects. *J. Clin. Invest*. 96:1859–1865. http://dx.doi.org/10.1172/JCI118231

Nydegger, S., S. Khurana, D.N. Krementsov, M. Foti, and M. Thali. 2006. Mapping of tetraspanin-enriched microdomains that can function as gateways for HIV-1. *J. Cell Biol*. 173:795–807. http://dx.doi.org/10.1083/jcb.200508165

Ono, A., and E.O. Freed. 2001. Plasma membrane rafts play a critical role in HIV-1 assembly and release. *Proc. Natl. Acad. Sci. USA*. 98:13925–13930. http://dx.doi.org/10.1073/pnas.241320298

Orenstein, J.M., M.S. Meltzer, T. Phipps, and H.E. Gendelman. 1988. Cytoplasmic assembly and accumulation of human immunodeficiency virus types 1 and 2 in recombinant human colony-stimulating factor-1-treated human monocytes: an ultrastructural study. *J. Virol*. 62:2578–2586.

Pelchen-Matthews, A., B. Kramer, and M. Marsh. 2003. Infectious HIV-1 assembles in late endosomes in primary macrophages. *J. Cell Biol*. 162:443–455. http://dx.doi.org/10.1083/jcb.200304008

Pelchen-Matthews, A., S. Giese, P. Mlčochová, J. Turner, and M. Marsh. 2012. β2 integrin adhesion complexes maintain the integrity of HIV-1 assembly compartments in primary macrophages. *Traffic*. 13:273–291. http://dx.doi.org/10.1111/j.1600-0854.2011.01306.x

Pomerantz, R.J., S.M. de la Monte, S.P. Donegan, T.R. Rota, M.W. Vogt, D.E. Craven, and M.S. Hirsch. 1988. Human immunodeficiency virus (HIV) infection of the uterine cervix. *Ann. Intern. Med*. 108:321–327. http://dx.doi.org/10.7326/0003-4819-108-3-321

Primo, L., C. Ferrandi, C. Roca, S. Marchiò, L. di Blasio, M. Alessio, and F. Bussolino. 2005. Identification of CD36 molecular features required for its in vitro angiostatic activity. *FASEB J*. 19:1713–1715.

Rahaman, S.O., D.J. Lennon, M. Febbraio, E.A. Podrez, S.L. Hazen, and R.L. Silverstein. 2006. A CD36-dependent signaling cascade is necessary for macrophage foam cell formation. *Cell Metab*. 4:211–221. http://dx.doi.org/10.1016/j.cmet.2006.06.007

Raposo, G., M. Moore, D. Innes, R. Leijendekker, A. Leigh-Brown, P. Benaroch, and H. Geuze. 2002. Human macrophages accumulate HIV-1 particles in MHC II compartments. *Traffic*. 3:718–729. http://dx.doi.org/10.1034/j.1600-0854.2002.31004.x

Rios, F.J.O., M.M. Koga, M. Ferracini, and S. Jancar. 2012. Co-stimulation of PAFR and CD36 is required for oxLDL-induced human macrophages activation. *PLoS ONE*. 7:e36632. http://dx.doi.org/10.1371/journal.pone.0036632

Roberts, W., S. Magwenzi, A. Aburima, and K.M. Naseem. 2010. Thrombospondin-1 induces platelet activation through CD36-dependent inhibition of the cAMP/protein kinase A signaling cascade. *Blood*. 116:4297–4306. http://dx.doi.org/10.1182/blood-2010-01-265561

Roesch, F., O. Meziane, A. Kula, S. Nisole, F. Porrot, I. Anderson, F. Mammano, A. Fassati, A. Marcello, M. Benkirane, and O. Schwartz. 2012. Hyperthermia stimulates HIV-1 replication. *PLoS Pathog.* 8:e1002792. http://dx.doi.org/10.1371/journal.ppat.1002792

Salahuddin, S.Z., R.M. Rose, J.E. Groopman, P.D. Markham, and R.C. Gallo. 1986. Human T lymphotropic virus type III infection of human alveolar macrophages. *Blood*. 68:281–284.

Savill, J., N. Hogg, Y. Ren, and C. Haslett. 1992. Thrombospondin cooperates with CD36 and the vitronectin receptor in macrophage recognition of neutrophils undergoing apoptosis. *J. Clin. Invest.* 90:1513–1522. http://dx.doi.org/10.1172/JCI116019

Sharova, N., C. Swingler, M. Sharkey, and M. Stevenson. 2005. Macrophages archive HIV-1 virions for dissemination in trans. *EMBO J.* 24:2481–2489. http://dx.doi.org/10.1038/sj.emboj.7600707

Sourisseau, M., N. Sol-Foulon, F. Porrot, F. Blanchet, and O. Schwartz. 2007. Inefficient human immunodeficiency virus replication in mobile lymphocytes. *J. Virol.* 81:1000–1012. http://dx.doi.org/10.1128/JVI.01629-06

Stuart, L.M., J. Deng, J.M. Silver, K. Takahashi, A.A. Tseng, E.J. Hennessy, R.A.B. Ezekowitz, and K.J. Moore. 2005. Response to *Staphylococcus aureus* requires CD36-mediated phagocytosis triggered by the COOH-terminal cytoplasmic domain. *J. Cell Biol.* 170:477–485. http://dx.doi.org/10.1083/jcb.200501113

Swerlick, R.A., K.H. Lee, T.M. Wick, and T.J. Lawley. 1992. Human dermal microvascular endothelial but not human umbilical vein endothelial cells express CD36 in vivo and in vitro. *J. Immunol.* 148:78–83.

Talle, M.A., P.E. Rao, E. Westberg, N. Allegar, M. Makowski, R.S. Mittler, and G. Goldstein. 1983. Patterns of antigenic expression on human monocytes as defined by monoclonal antibodies. *Cell. Immunol.* 78:83–99. http://dx.doi.org/10.1016/0008-8749(83)90262-9

Tan, J., and Q.J. Sattentau. 2013. The HIV-1-containing macrophage compartment: a perfect cellular niche? *Trends Microbiol.* 21:405–412. http://dx.doi.org/10.1016/j.tim.2013.05.001

Tandon, N.N., U. Kralisz, and G.A. Jamieson. 1989. Identification of glycoprotein IV (CD36) as a primary receptor for platelet-collagen adhesion. *J. Biol. Chem.* 264:7576–7583.

Taylor, P.R., L. Martinez-Pomares, M. Stacey, H.-H. Lin, G.D. Brown, and S. Gordon. 2005. Macrophage receptors and immune recognition. *Annu. Rev. Immunol.* 23:901–944. http://dx.doi.org/10.1146/annurev.immunol.23.021704.115816

Wang, J.-H., C. Kwas, and L. Wu. 2009. Intercellular adhesion molecule 1 (ICAM-1), but not ICAM-2 and -3, is important for dendritic cell-mediated human immunodeficiency virus type 1 transmission. *J. Virol.* 83:4195–4204. http://dx.doi.org/10.1128/JVI.00006-09

Welsch, S., O.T. Keppler, A. Habermann, I. Allespach, J. Krijnse-Locker, and H.-G. Kräusslich. 2007. HIV-1 buds predominantly at the plasma membrane of primary human macrophages. *PLoS Pathog.* 3:e36. http://dx.doi.org/10.1371/journal.ppat.0030036

Welsch, S., F. Groot, H.-G. Kräusslich, O.T. Keppler, and Q.J. Sattentau. 2011. Architecture and regulation of the HIV-1 assembly and holding compartment in macrophages. *J. Virol.* 85:7922–7927. http://dx.doi.org/10.1128/JVI.00834-11

Wolf, Z., E. Orsó, T. Werner, H.H. Klünemann, and G. Schmitz. 2007. Monocyte cholesterol homeostasis correlates with the presence of detergent resistant membrane microdomains. *Cytometry A.* 71:486–494.

Zeng, Y., N. Tao, K.-N. Chung, J.E. Heuser, and D.M. Lublin. 2003. Endocytosis of oxidized low density lipoprotein through scavenger receptor CD36 utilizes a lipid raft pathway that does not require caveolin-1. *J. Biol. Chem.* 278:45931–45936. http://dx.doi.org/10.1074/jbc.M307722200

Zhang, J., and I. Crandall. 2007. Expression of both N- and C-terminal GFP tagged huCD36 and their discrepancy in OxLDL and pRBC binding on CHO cells. *Lipids Health Dis.* 6:24. http://dx.doi.org/10.1186/1476-511X-6-24